POLITECNICO DI TORINO

Master Degree in Mechatronic Engineering

2019/2020

MASTER DEGREE THESIS

Smart Shock Absorber:
Design, Development and Testing

Thesis Student:
Gianluca D'Ereditá - s242400

Professor:
Prof. Maizza Giovanni

Contents

Chapter 1

Introduction

Vibration is an important part in mechanical analysis systems, which can be found in every automotive engineering problem. Vibration is a mechanical phenomenon whereby oscillations occur through an equilibrium point. It can be occurred in two ways, either, when a mechanical system is set off with an initial input and then allowed to vibrate freely that is called free vibration or when an alternating force or motion is applied to a mechanical system that is called force vibration.
Vibration force is the main factor in the analysis of moving vehicles, because, the forces which are imposed throughout the chassis by the road cause vibration. Suspension system of a vehicle has an important role in damping vibration of a vehicle. Due to the linkage between the tires and chassis, hence, every force which is imposed to the tires by the humps of the road will be transferred to the chassis. This fact has been made suspension system as an important part during vibration analysis of the vehicle.
During operation of suspension system, when the vehicle is moving, all parts of suspension system are vibrating with specific angular velocity and acceleration. This dynamic condition in suspension system causes dynamic forces which cause stress on different parts of suspension system, especially on lower arm of suspension system. In order to determine this stress on the lower arm, dynamic analysis must be done on suspension system. It must be mentioned that each suspension system has contained different parts, where one of them is the lower arm which has important role in operation of suspension system.
This study has 2 main parts that are Finite Element Analysis and Experimental Analysis. The Finite Element Analysis has been performed using the software called Solidworks, then in order to validate the results come from the finite element analysis, the Experimental analysis has been performed using a test rig.

Problem Definition

The rough surface road profiles and its influence on vehicle, causing unwilling vibrations due to kinematic excitations, have been made destructive problems on suspension system of vehicle. Respectively, every part of the suspension system will be affected by destructive created vibration. The lower drive arm of a suspension system is mainly influenced by this condition.
Moreover, Increasing in load condition on the lower arm of suspension system can change distribution of stress. Hence, these unpleasant vibration and force conditions will reduce life time of lower arm, by creating physical damage due to stress. Therefore, vibration and force analysis of this part will be helpful to make a better operation condition for

suspension system. The main problems due to vibration and load conditions on lower arm of suspension system can be defined as follow:

- Imposed force to the vehicle by the road has important role in load condition of suspension system, specially, on its lower arm. Increasing in this load may cause to increase stress on lower arm. Hence, trying to reduce this force is considerable. The value of road force depends on specific conditions such as quality of the road, velocity and acceleration of vehicle. There are other conditions that can affect this force; these conditions are related to physical condition of suspension system and vehicle tire such as: suspension stiffness, suspension damping coefficient, tire stiffness and suspension system mass.

- Reaction forces on suspension system, also, play an important role in load and stress conditions of lower arm. These forces are imposing to lower arm from the chassis (the lower arm is fixed to the chassis) and from other parts which are connected to it. Figure below describes the problem conditions on lower arm of suspension system.

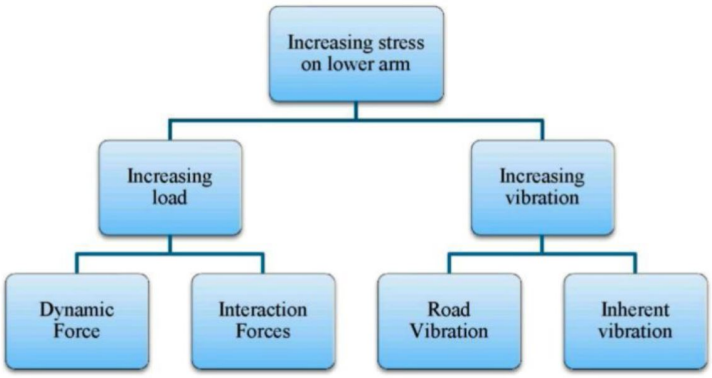

General problems of suspension system of a moving vehicle can be divided in two categories. The first one is related to problems of stress on different parts of suspension system and the second one is related to destructive vibration on suspension system.

Objective

The main goal of this study is to evaluate the life of the Lower Control, in order to estimate it the life strain method has been applied.

Methodology

The methodology in this study can be divided in three main topic: Design, Calculation and Simulation. The Design Part can be divided in more subpart such as Model of the Wheel, Design of all component, assembling of all component. The calculation Part and the Simulation one goes together because in order to have stress and strain of the lower control arm we have to simulate different input then use this stress/strain to do the calculation and in the end plot all the results.

Design

In order to start the simulation the first goal is to model the wheel in order to be more similar to the real one.
in order to do this I supposed the system as a 2 DOF quarter car model and then using the paper called "Dynamic Simulation of Vehicle Suspension Systems for Durability Analysis" made by Levesley, M.C., Kember S.A., Barton, D.C., Brooks, P.C., Querin, O.M [1] i used the damping coefficient and stifness constant of a wheel.

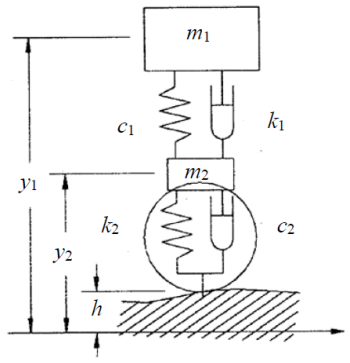

	Symbol	Value
Tyre Stiffness Constant $\left[\frac{kN}{m}\right]$	K_2	200
Tyre Damping Coefficient $\left[\frac{kNs}{m}\right]$	c_2	0.1
Suspension Stiffness Constant $\left[\frac{kN}{m}\right]$	K_2	20
Suspension Damping Coefficient $\left[\frac{kNs}{m}\right]$	c_2	1

Where:

- m_1: mass of the quarter quad model;
- c_1: damping coefficient of the suspension;
- K_1: Stifness constant of the suspension;
- m_2: mass of wheel;
- c_2: damping coefficient of the Tyre;
- K_2: Stifness constant of the Tyre;

The next step is to design a test rig that is more similar to the real one in order to perform a precise simulation on the studied parts.
And in the end we must design all the other parts according with the geometry of the real quad. Then before starting for the simulation we must choose fpr the material.

Main Support The Main support is the part that is fixed to the machine it simulates the connection of the lower arm and of the suspension system to the chassy of the car, in our case of the quad.

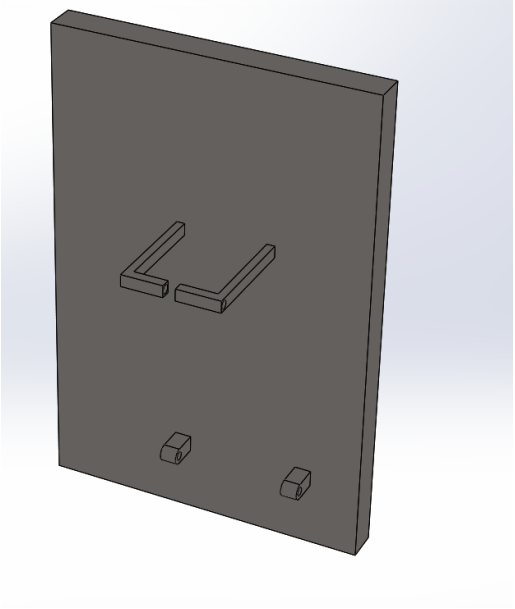

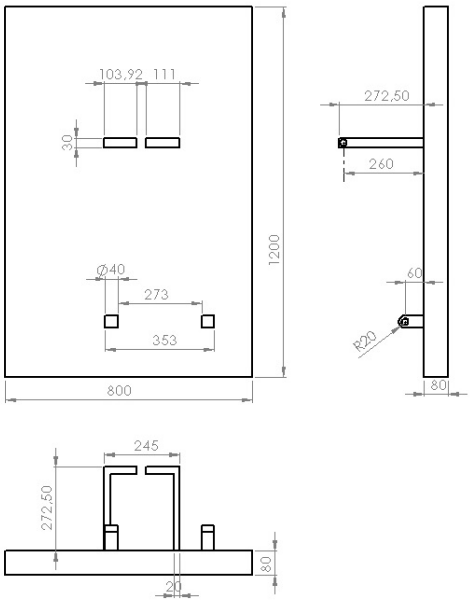

Lower Arm This part has the design taken from the real piece. It is the center of the study.

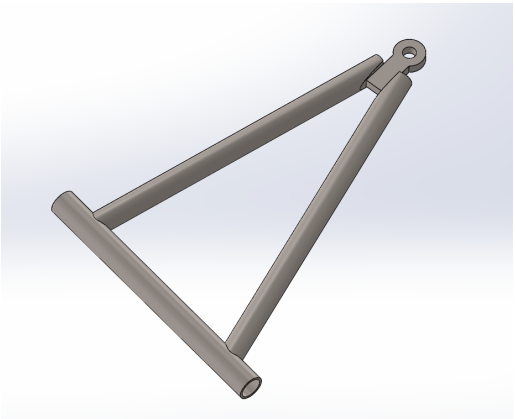

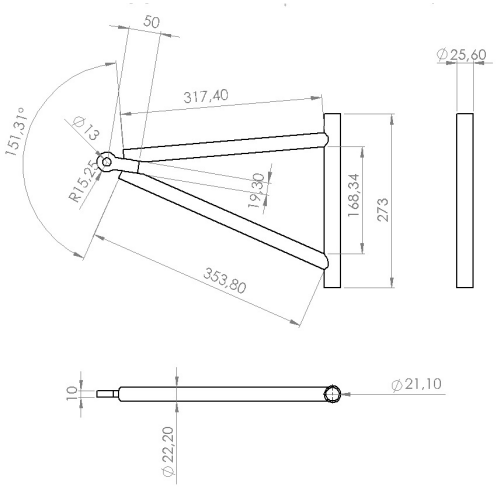

Damper Also this component is designed from the real one, using the real measurements, then all the parameter such as damping factor and stiffness have been simulated using the software. The Damper is assembled from the rod and from the tube.

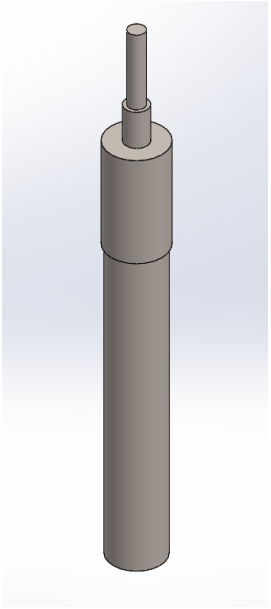

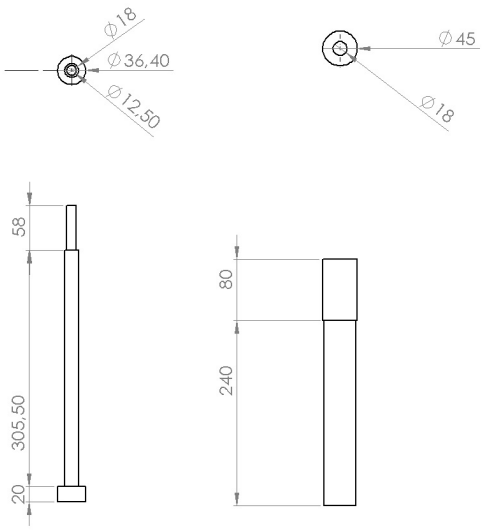

Knuckle This is the connection between the damper and the lower arm and also this component has been designed from the real data.

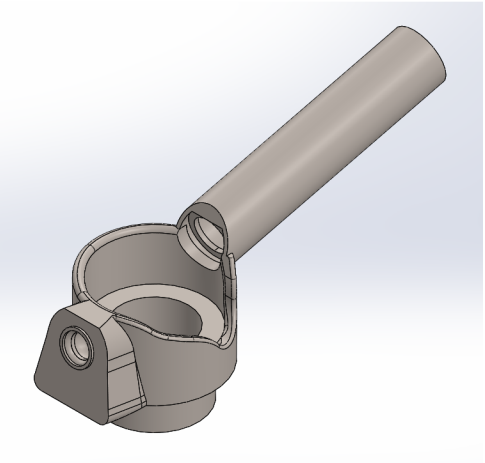

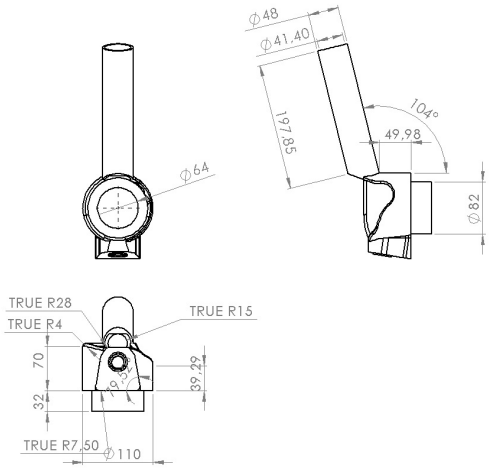

Accessories In this part we have all that part that are use to connect 2 part in order to simulate the movement, or to lock the component in a particular position such as the real position.

Ball Pin

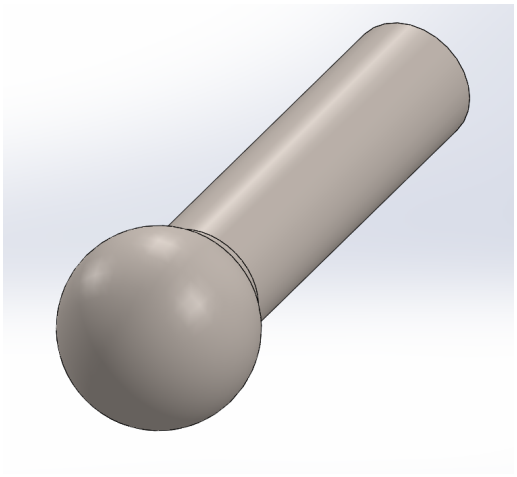

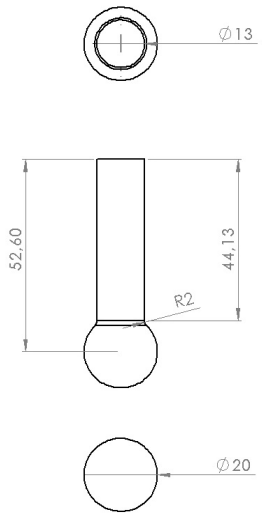

Cap

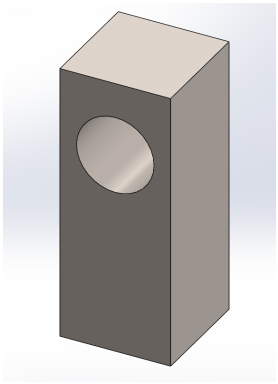

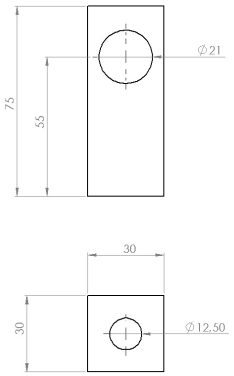

Assembly Joining all the component in one file we obtain this assembly.

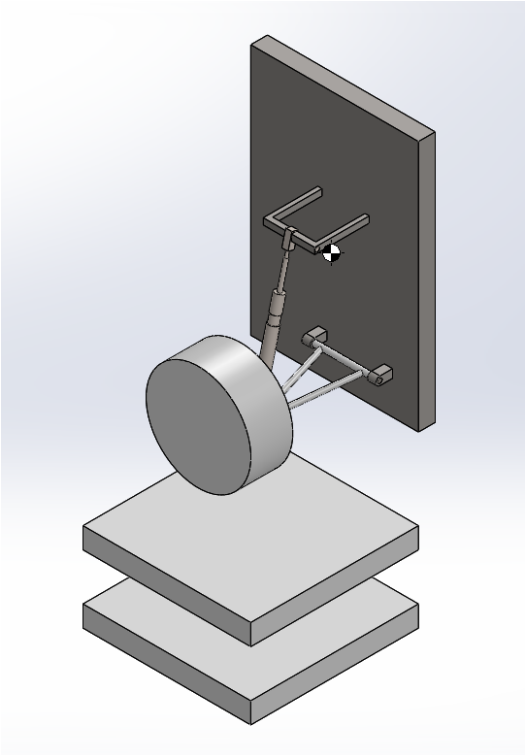

Material

For the material i followed the instuction of the paper called "Fatigue Life Prediction of Lower Suspension Arm Using Strain-Life Approach" [2] made by "Prof. Dr. Md. Mustafizur Rahman, Kumaran Kadirgama, M.M. Noor, Ruzaimi Rejab" in which they say that Aluminium 6082-T6 is one the aluminium alloys that is used in automotive to do lower arm, then to do a comparison i choose another material that is used in automotive to craft that component: Steel S355.

Aluminium 6082-T6

6082 aluminium alloy is an alloy in the wrought aluminium-magnesium-silicon family (6000 or 6xxx series). It is one of the more popular alloys in its series (alongside alloys 6005, 6061, and 6063), although it is not strongly featured in ASTM (North American) standards. It is typically formed by extrusion and rolling, but as a wrought alloy it is not used in casting. It can also be forged and clad, but that is not common practice with this alloy. It cannot be work hardened, but is commonly heat treated to produce tempers with a higher strength but lower ductility.
Alternate names and designations include AlSi1MgMn, 3.2315, H30, and A96082.

Chemical Composition (According to EN 573.3):

	Si	Fe	Cu	Mn	Mg	Cr	Zn	Ti
% weight	$0.7 \div 1.3$	0.5 max	0.1 max	$0.4 \div 1$	$0.6 \div 1.2$	0.25 max	0.2 max	0.1 max

Properties:

- Density: 2.71 $\frac{g}{cm^3}$
- Young's modulus: 71 GPa
- Ultimate tensile strength: 140 to 330 MPa
- Yield strength: 280 MPa
- Thermal Expansion: 23.1 $\mu m/m - K$.
- Solidus: 575 °C

Steel s355

Steel is an alloy of iron with typically a few percent of carbon to improve its strength and fracture resistance compared to iron. The name of different steel change for which purpose they are used for.

Application Symbol	Meaning
S	Structural Steel
P	Steel for pressure lines and vessels
L	Steel for pipe and tube
E	Engineering Steels
B	Steel for reinforced concrete
R	Steel for Rail use
H	High Tensile strength Fiat products
D	Fiat Products for Cold Forming
T	Tinmill Products
M	Electrical Steel

So in our case the steel is designed for structural purpose.
The next set of 3 digits gives the steel's minimum yield strength. In our case is 355 MPa

Chemical Composition (according to EN 10025-2):

	C	Mn	P	S	Si
% of weight	0.23 max	1.6 max	0.05 max	0.05 max	0.05 max

Properties:

- Density: 7.85 $\frac{g}{cm^3}$
- Young's modulus: 210 GPa
- Ultimate tensile strength: from 470 to 510 MPa
- Yield strength: 355 MPa
- Thermal Expansion: 12 $\mu m/m - K$.
- Poisson Ratio: 0.3

Analysis

After the design of the test rig, assembly of all componenent designed and the choice of the material, the next step is Analysis.

Motion Analysis

The aim of this section is to evaluate the stress and strain in the lower arm when difference input are applied. For the simulation I used different scenarios
The scenarios applied are 2:

- Road Profile of the type C
- Three different Road bump

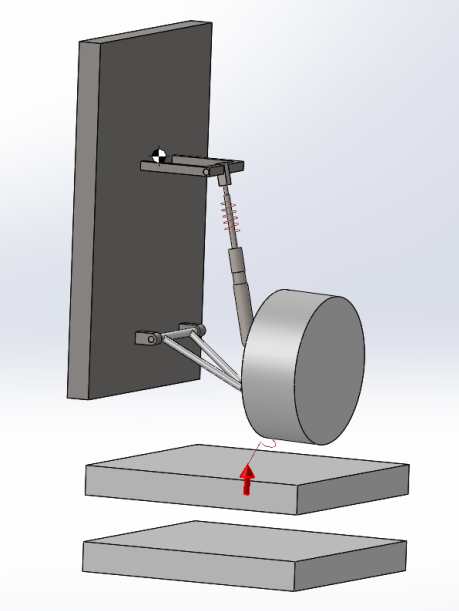

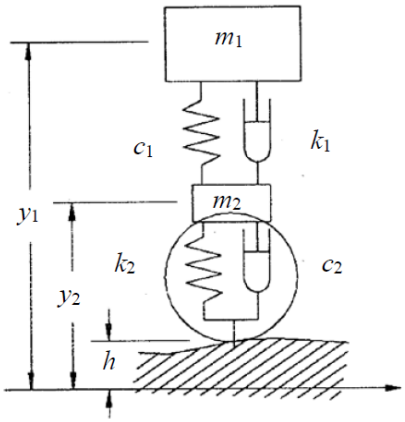

This is the Model that I used for the Simulation. The two box on the lower part represents the contact point of the wheel with the road, and it is a way to represent the distance h in the different scenarios. The other coefficient such m_1 or m_2 as been choosen according to the datasheet of the quad under inspection, "Polaris Sportsman 800 EFI".

Road Profile

The Road profile has been generated according the "ISO 6808:2016 Mechanical vibration — Road surface profiles" where there are different classification of raod.
The road profile can be represented by a PSD function.
The power spectral densities of roads show a characteristic drop in magnitude with the wave number. To determine the power spectral density function, or PSD, it is necessary to measure the surface profile with respect to a reference plane. Random road profiles can be approximated by a PSD in the form of

$$\Phi(\Omega) = \Phi(\Omega_0)\left(\frac{\Omega}{\Omega_0}\right)^{-w} \text{ or } \Phi(n) = \Phi(n_0)\left(\frac{n}{n_0}\right)^{-w}$$

Where:

- $\Omega = \frac{2\pi}{L}$ in $\frac{rad}{s}$ denotes the angular spatial frequency, L is the waveleghth,
- $\Phi_0 \triangleq \Phi(\Omega_0)$ in $\frac{m^2}{\frac{rad}{m}}$ describes the values of the psd at the reference wave number $\Phi_0 = 1\ \frac{rad}{m}$,
- $n = \frac{\Omega}{2\pi}$ is the spatial frequency, $n_0 = 0.1\ \frac{cycle}{m}$,
- w is the waviness, for most of the road surface, w=2;

Road Roughness values classified by ISO						
	Degree of Roughness					
	$\Phi(n_0)\left(\frac{10^{-6}m^2}{\frac{cycle}{m}}\right)$ where n_0=0.1$\frac{cycle}{m}$			$\Phi(\Omega_0)\left(10^{-6}m^3\right)$ where $\Omega_0 = 1\frac{rad}{m}$		
Road Class	Lower limit	Mean	Upper Limit	Lower limit	Mean	Upper Limit
A (very good)	-	16	32	-	1	2
B (good)	32	64	128	2	4	8
C (average)	128	256	512	8	16	32
D (poor)	512	1024	2048	32	64	128
E (very poor)	2048	4096	8192	128	256	512

Road Profiles in Spatial and Temporal Domain

It is well known that the amount of road excitation imposed at the vehicle tire depends on two factors:

- The road roughness which is a function of the road roughness coefficient,
- the vehicle velocity V

Let s be the path variable. By introducing the wavelength

$$\lambda = \frac{2\pi}{\Omega}$$

and assuming that s=0 at t=0, the term Ωs can be written as

$$\Omega s = \frac{2\pi}{\lambda} s = 2\pi \frac{V}{\lambda} t = \omega t$$

where $\omega\ \frac{rad}{s}$ is the angular velocity in time domain, we end up with

$$\Omega V = \omega$$

Hence, in the time domain the excitation frequency is given by $f = \frac{\omega}{2\pi} = \frac{V}{\lambda}$. For most of the vehicles the rigid body vibrations are in between $f = 0.5Hz$ to $f = 15Hz$. This range is covered by waves which satisfy the conditions $0.5Hz \leq \frac{v}{\lambda} \leq 15Hz$. Hence, to achieve an excitation in the whole frequency range with moderate vehicle velocities profiles with

different varying wavelengths are needed.
When a vehicle is moving along the road with velocity V, the excitation frequency of the road input $\omega \left(\frac{rad}{s}\right)$ becomes $\omega = \Omega V$. The mean squared value of road surface roughness, that is the total area of the power spectral density function, does not change with the velocity of a vehicle. Let $\Psi(\omega)$ represents the power spectral density of road input with respect to displacement excitation frequency. Therefore we have the following relation:

$$\Psi(\omega)d\omega = \Phi(\Omega)d\Omega$$

which in turn yields the relationship between $\Psi(\omega)$ and $\Phi(\Omega)$

$$\Psi(\omega) = \Phi(\Omega)\frac{1}{V}$$

Henceforth, we have

$$\Psi(\omega) = \Phi(\Omega_0)\Omega_0^2\frac{V}{\omega^2}$$

This indicates that the road profile can be obtained from integrating a white noise in time domain. While to prevent standard deviation from going up with time as the integration period is increased. The road roughness PSD distribution is modified as

$$\Psi(\omega) = \frac{2\alpha V\sigma^2}{\omega^2 + \alpha^2 V^2}$$

where

- σ^2 denotes the road roughness variance and V the vehicle speed, whereas
- α depends on the type of road surface.

Since the spectral density of the road profile can be factored as

$$\Psi(\omega) = \frac{2\alpha V\sigma^2}{(\alpha V + j\omega)(\alpha V - j\omega)} = H(\omega)\Psi_w H^T(-\omega)$$

where

- $H(\omega) \triangleq \frac{1}{\alpha V + j\omega}$is the frequency response function of the shaping filter,
- $\Psi_w \triangleq 2\alpha V\sigma^2$ is the spectral density of a white noise process.

Hence, if the vehicle runs with constant velocity $\frac{ds}{dt} = V$, then the road profile signal, $z_R(t)$, whose PSD is given by the previous formula, may be obtained as the output of a linear filter expressed by the differential equation

$$\frac{d}{dt}z_R(t) = -\alpha V z_R(t) + \omega(t)$$

Road Roughness values classified by ISO			
	Degree of Roughness		
Road Class	σ (10^{-3})	$\Phi(\Omega_0)$ $(10^{-}6m^3), \Omega_0 = 1$	α $\frac{rad}{m}$
A (very good)	2	1	0.127
B (good)	4	4	0.127
C (average)	8	16	0.127
D (poor)	16	64	0.127
E (very poor)	32	256	0.127

From this last equation we can build using Simulink a model that can give us the road profile.

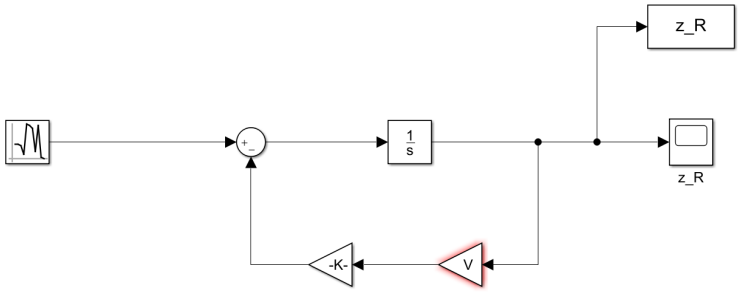

The results of the simulation generates this output:

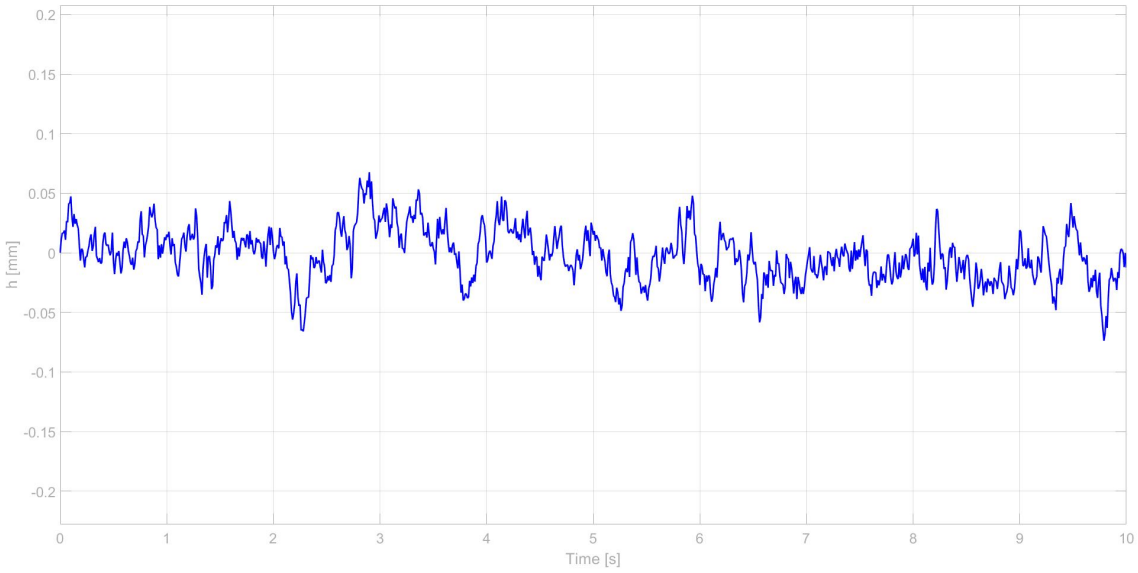

The other input are the road bump present on the italian roads and regulated by the "(Art. 42 Cod. Str.) Rallentatori di velocità", that says:

- On the road where the max velocity is 50 Km/h, the width is 60 cm and the height is 3 cm
- On the road where the max velocity is 40 Km/h, the width is 90 cm and the height is 5 cm

- On the road where the max velocity is 30 Km/h, the width is 120 cm and the height is 7 cm

I modelled them using a sine function and a trapezoidal function on matlab and then imported them in Solidworks. This is the results:

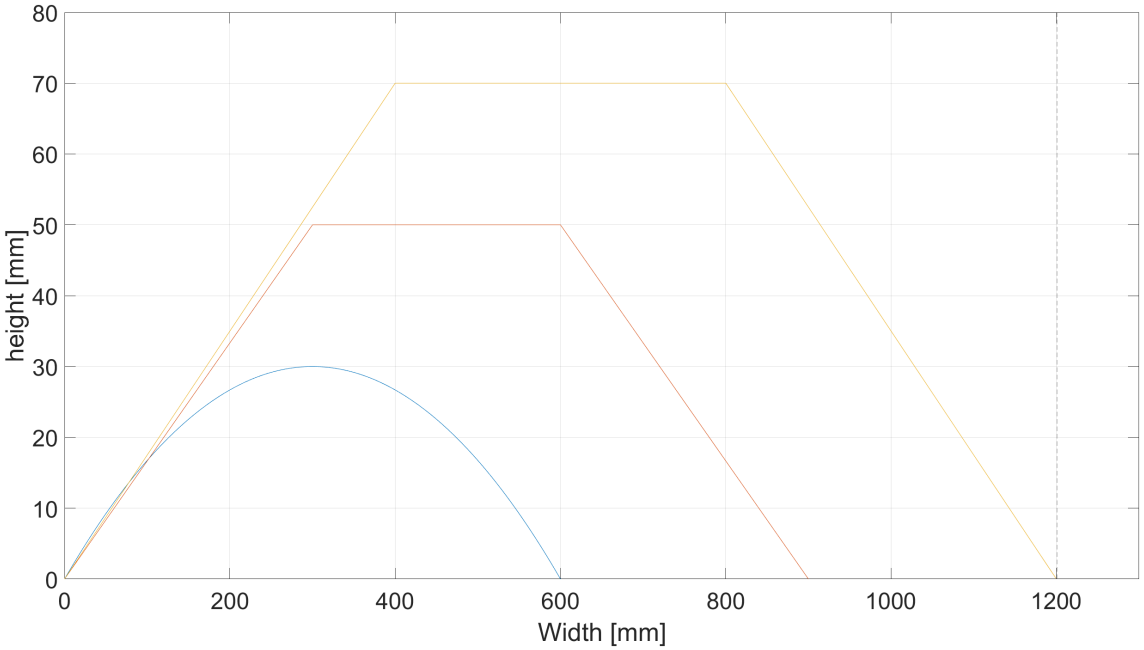

In the figure below it can be seen all the setup for the simulation.

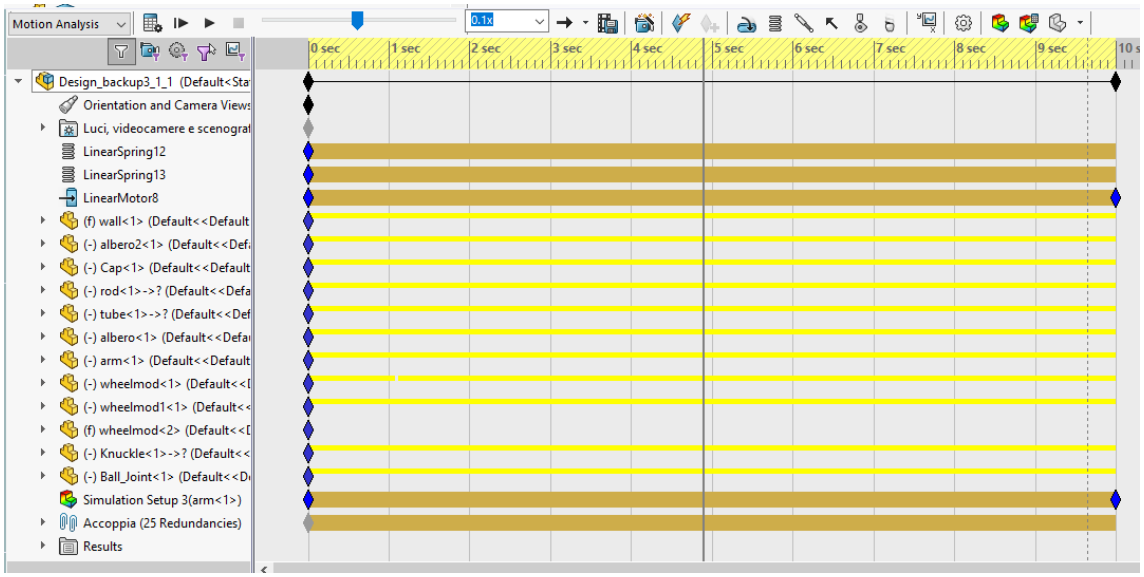

Chapter 2

Literature Review

Suspension System

Suspension is the term given to the system of springs, shock absorbers and linkages that connects a vehicle to its wheels and allows relative motion between the two parts.
Suspension systems serve a dual purpose contributing to the vehicle's road holding, handling and braking for active safety and driving pleasure. In addition, Suspension systems are used for keeping vehicle occupants comfortable and reasonably well isolated from road noise, bumps, and vibrations.

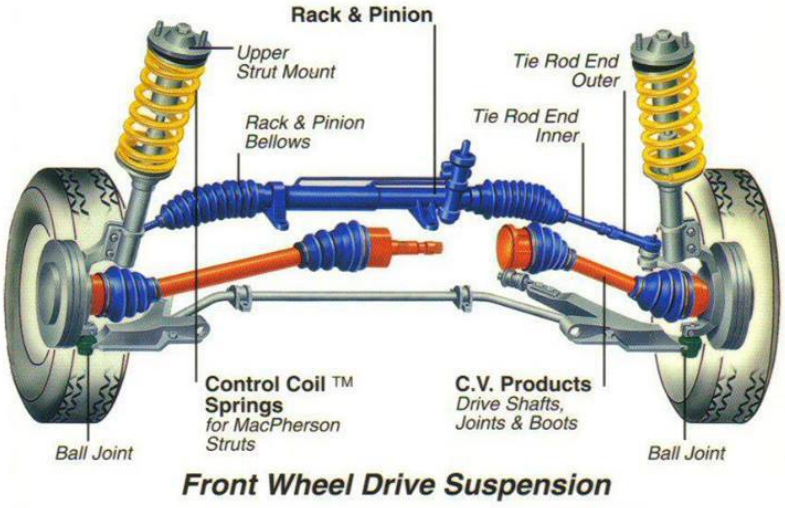

These goals are generally at odds, so the tuning of suspensions involves finding the right compromise. It is important for the suspension to keep the road wheel in contact with the road surface as much as possible, because the road forces are acting on the vehicle through the contact patches of the tires.
The main functions of suspension system are as follows:

- To protect vehicle from road shocks
- To safeguard passengers from shocks
- To prevent pitching and rolling

According to the design, suspension system is mainly classified into two types, which are dependant suspension system and independent one. Regarding to dependant suspension system, a beam holds the wheels parallel to each other and perpendicular to the axle. When the camber of one wheel changes, the similarly camber of opposite wheel also changes. In contrary, independent suspension points to each wheel having its own suspension; it won't upset the wheel of the axle if the opposite wheel has been experienced. In other words, it can be mentioned that both the front and the rear wheel are utilized; when one wheel goes down, the other wheel does not have much effect.
Comfort and control aspects are majors in field of design and manufacturing. Spring and damper systems are used as shock absorber in automobiles. As concerned to comfort and control aspects, their systems are lagging to provide optimum level of performance.
The geometry of suspension system does this optimum level of performance by providing automatic compensation that minimizes deviations caused by external forces.
The automobile chassis is generally mounted on the axle through springs. These springs are used to prevent the vehicle body from shock which refers to bounce, pitch and roll, etc. Due to these shock frames, body is affected by additional stresses which affect indirectly on rider to feel some discomfort.
In a moving vehicle, a proper suspension system must satisfy some duties which are considered to prevent vehicle from road shocks, to safeguard passengers from shocks and to prevent pitching or rolling. Springs are placed between the wheels and body; when wheels come across the bumps on road, it rises and deflects the spring. Thus, energy is stored and released when the spring rebounds due to its elasticity. Gradually the amplitude decreases due to the friction between spring and joints. Also, It must keep tires in contact with road.

Dynamic Analysis

Vector analysis mostly has been used to express dynamic behavior of mechanical systems, as well as, suspension system. This method can develop the understanding of suspension operation and its effects on total vehicle performance. The calculations for dynamic analysis will include a series of analyses including:

- Velocity analysis
- Acceleration analysis
- Dynamic force analysis

Most practical vehicles have some form of suspension, particularly when there are four or more wheels. The suspension system in general must reduce the vertical wheel load variations which are imposed to the wheel by bumps of the road. However, the introduction of a suspension system introduces some tasks of its own; each additional interface and component brings some specific load condition for suspension system during its operation. These three categories are considered as an important load condition of suspension system that has been encountered: wheel load variation, handling load and component loading environment.
In order to determine the wheel load variation in a vehicle, it is possible to assign specific stiffness to each wheel and suspension of each tire and model vehicle as sprung and un-sprung mass to determine the load. It must be mentioned that the calculated load completely depends on the profile of the load. For handling force, the distribution of loads

between sprung and un-sprung load paths have an important role. Therefore an anti-pitch angle will be defined in order to reduce the load between sprung and un-sprung in different manoeuvres of the vehicle. In the third part, component loading, each part of the suspension 0system due to both speed and acceleration of the vehicle and imposed forces will have interactions to each other. These interactions cause forces on each joints.
In order to analyze the lower arm of suspension system by finite element software, its load condition must be determined. Hence, imposed forces on the lower arm created by the other parts of the suspension system must be determined. the figure below shows McPherson suspension system. All of components of McPherson suspension system have been showed as well.

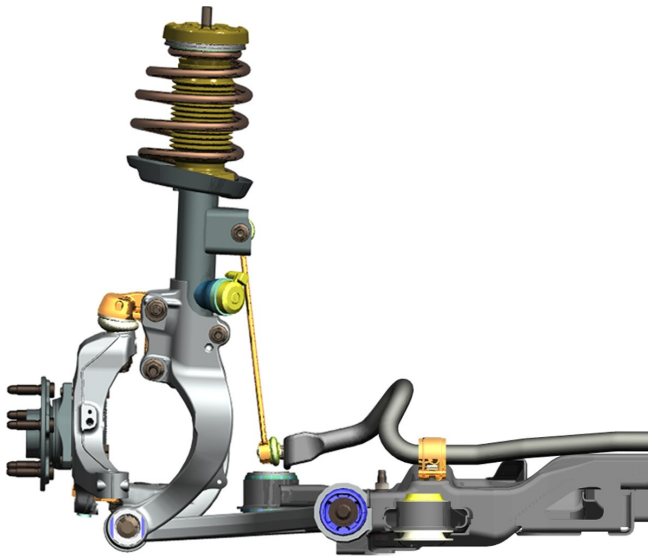

The imposed forces on lower arm are due to interaction of other parts with lower arm.
Hence the first step in force analysis has been related to both velocity and acceleration analysis on suspension system. For velocity analysis, a starting point will be set on contact point between the tire and the road in order to establish a boundary condition. The position, velocity and acceleration of starting point, respectively depends on the profile of the road and velocity and acceleration of the vehicle.
The usual method for analysis component of suspension system is vector analysis used to determine their velocity, acceleration and dynamic forces. For proceeding with velocity and acceleration analysis, it is necessary to identify the unknowns that define the problem and the same number of equations as unknowns leading to solution. The angular velocity will be assigned to the each rigid body of suspension system and a rotating velocity in the attachment of lower arm to the chassis of the vehicle.
There is also the same assumption for acceleration analysis of suspension system. By determining velocity and acceleration of lower arm and other components of suspension system, dynamic force analysis of suspension system is not unavoidable. Specifically for the lower arm of suspension system, six equations of motions will be set up. The dynamic analysis depends on the physical properties of suspension components like mass, mass moments of inertia and center of mass location.

Strain Life Approach

The Strain Life approach is used to predict the how long a component will survive due to cyclic loading.
Strain Life differs from other approaches to fatigue because it takes into account both the elastic and plastic deformation of a material. Some approaches, like Stress Life, are only suitable when the stresses and strains remain in the elastic region of a material.
To understand how strain life fatigue calculations work, it is helpful to understand the relationship between stress and strain. When a load is applied over an area, it creates stress. This stress in turn creates a strain, or elongation, as the part deforms.

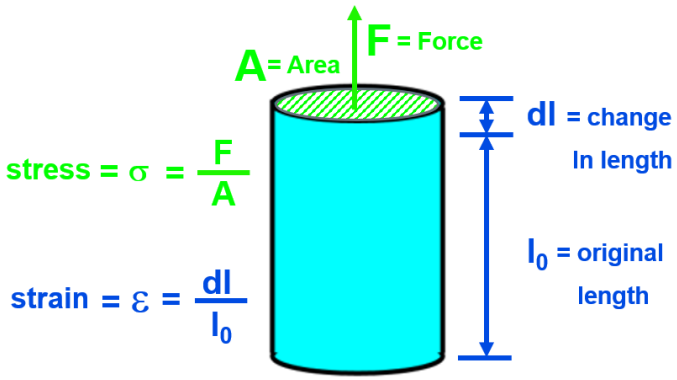

Subjected to cyclic stresses over time during usage, permanent deformation (when the part does not return to its original length when the load is removed) can occur. n fact, the stress and strain may not maintain a linear relationship.
Eventually enough cycles can be applied that the part fails (i.e., a crack forms, or object cannot carry a load). To understand when this failure could occur, it is necessary to understand the non-linear relationship between stress and strain. At low stress levels, the relationship of stress to strain is linear (i.e., elastic) and related by the Young's Modulus of the material. At higher stress levels, the stress to strain relationship is not linear (i.e., plastic). The Strain Life approach utilizes both elastic and plastic behavior.
Starting with a measured strain, the strain life approach takes the following steps:

- A corresponding stress at the same location as the measured strain is calculated.
- This creates a local stress-strain time history which is cycle counted by plotting the stress against the strain.
- The strain cycles are converted to damage to calculate the fatigue life using the Manson-Coffin-Morrow Strain Life curve (also called an ϵ-N Curve). This should also include effects of mean stress.

In order to calculate fatigue damage, the corresponding stress at the same location of the measured strain is needed. The Ramberg-Osgood relationship can be used to calculate the corresponding stress. The local stress-strain time history can only predict the life at the location of the measurement. It cannot predict the life based on any other location. The Ramberg-Osgood relation is an equation that describes the non-linear relationship between stress and strain, including materials that harden with plastic deformation. The 2 graph below represents the stress-strain graph in both region, plastic and elastic, using the Ramberg-Osgood Relation.

$$\epsilon = \frac{\sigma}{E} + \left(\frac{\sigma}{K'}\right)^{\frac{1}{n'}}$$

where

- ϵ is the strain amplitude
- σ is the amplitude of stress cycle
- E is the young's Modulus
- n' is cyclic hardening exponent
- K' is cyclic hardening coefficient

Material	K' [Mpa]	n'
Aluminium 6082-T6	587.5	0.203
Steel S355	630.6	0.1085

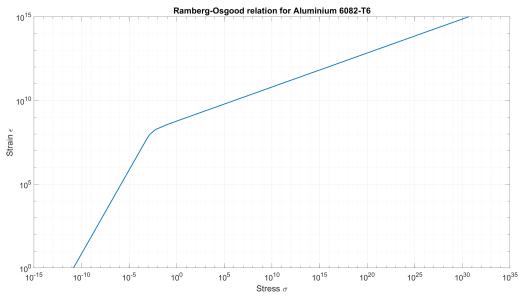

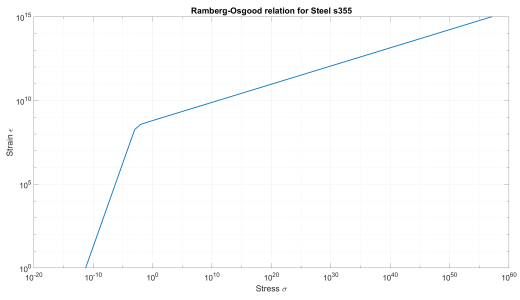

A comparison between the two relation

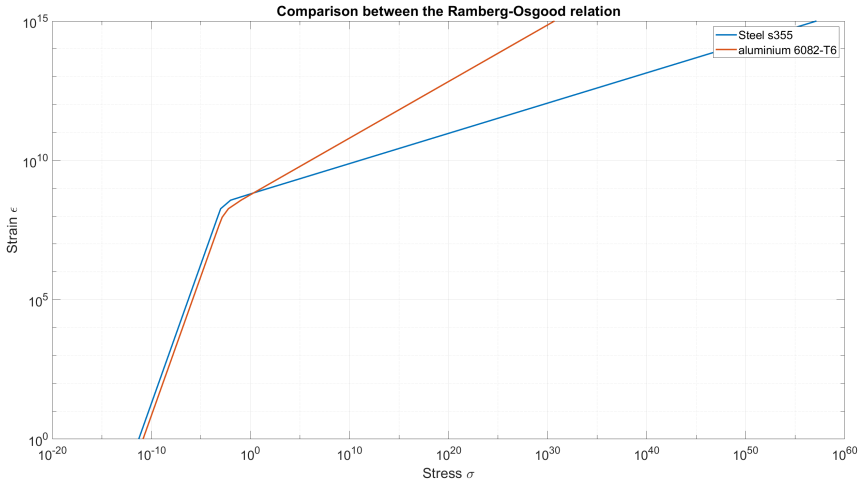

The number and amplitude of potentially damaging cycles in the local stress-strain history need to be determined from the operating data. This is done by plotting the local stress-strain time history blocks against each other.

Rainflow Counting Method

The rainflow-counting algorithm is used in the analysis of fatigue data in order to reduce a spectrum of varying stress into an equivalent set of simple stress reversals. The method successively extracts the smaller interruption cycles from a sequence, which models the material memory effect seen with stress-strain hysteresis cycles. This simplification allows the fatigue life of a component to be determined for each rainflow cycle using either Miner's rule to calculate the fatigue damage, or in a crack growth equation to calculate the crack increment.
The rainflow method is compatible with the cycles obtained from examination of the stress-strain hysteresis cycles. When a material is cyclically strained, a plot of stress against strain shows loops forming from the smaller interruption cycles. At the end of the smaller cycle, the material resumes the stress-strain path of the original cycle, as if the interruption had not occurred. The closed loops represent the energy dissipated by the material.

Manson-Coffin-Morrow Curve and Damage Calculation

The Manson-Coffin-Morrow Strain Life curve (also called a ϵ-N curve) characterizes the number and amplitude of strain cycles a material can take before failing.

$$\epsilon_a = \frac{\sigma'_f}{E}(2N)^b + \epsilon'_f(2N)^c$$

where

- ϵ_a is the strain amplitude
- N is the number of cycles to failure
- b is the fatigue strength exponent
- c is the fatigue ductility exponent
- E is the Young's Modulus
- ϵ'_f is the ductility coefficient
- σ'_f is the strength coefficient

Material	b	c	E	ϵ'_f	σ'_f
Aluminium 6082-T6	-0.07	-0.593	70 GPa	0.209	486.8 MPa
Steel S355	-0.09	-0.616	190 Gpa	0.608	912 MPa

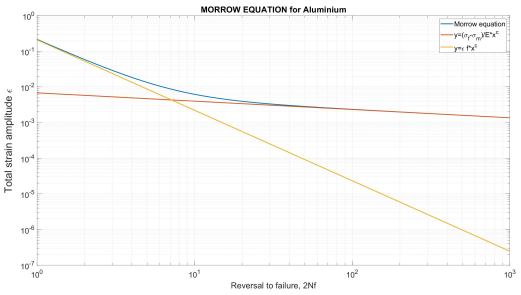

A comparison between the two relation

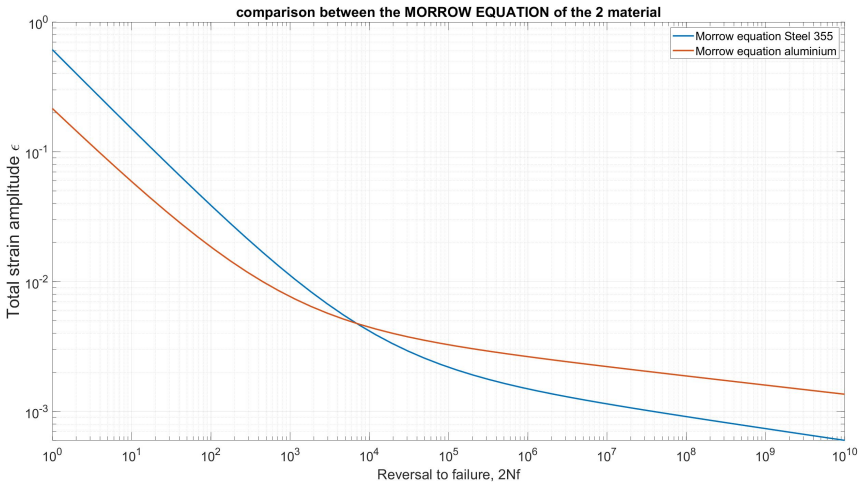

The strain-life curve (also referred to as the ϵ-N curve) is property of the material itself. It contains both an elastic portion (Red line above) and a plastic portion (yellow line above). It relates the total cyclic amplitude (blue line above) of the strain cycle to the number of cycles until the part fails. It is similar in concept to the SN Curve used in stress life calculations.

Then the intercept of the total strain amplitude of the cycle with the Manson-Coffin-Morrow Curve gives the expected life.

Smith-Watson-Topper Curve and Damage Calculation

It differs from the Manson-Coffin-Morrow Curve because it takes into accounts max stress. Thus the Equation became:

$$\sigma_{max}\epsilon_a E = \sigma_f'^2(2N)^{2b} + \sigma_f'\epsilon_f'(2N)^{b+c}$$

- ϵ_a is the strain amplitude
- N is the number of cycles to failure
- b is the fatigue strength exponent
- c is the fatigue ductility exponent
- E is the Young's Modulus
- ϵ_f' is the ductility coefficient
- σ_f' is the strength coefficient
- σ_{max} is the max stress

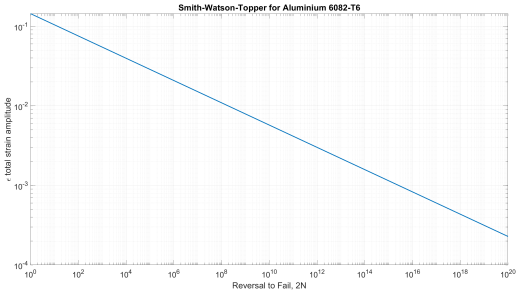

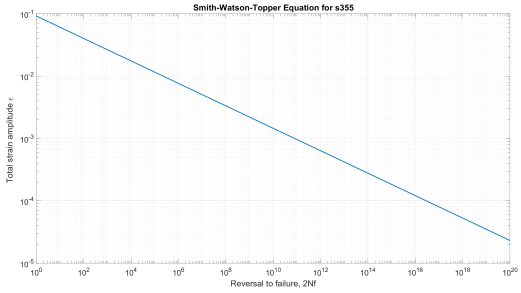

Chapter 3

Instrumentation

Universal Measuring Amplifier

QuantumX MX840B

QuantumX MX840B

QuantumX MX840B is a 24-bit Universal Measuring Amplifier, that has special features like:

- 8 invidually configurable measurement channels (Galvanic isolated)
- Connection of more than 16 differenttransducer technologies per channel
- Individual sample rates up to $40kS/s$ perchannel, active low pass filter
- 24-bit A/D converter per channel
- Automatic channel parameterization(TEDS[1])
- Supply voltage for active transducers(DC): $5V \div 24V$
- CANbus Input/Output

[1]TEDS: transducer electronic data sheet; A transducer electronic data sheet (TEDS) is a standardized method of storing transducer (sensors or actuators) identification, calibration, correction data, and manufacturer-related information.

Block Diagram

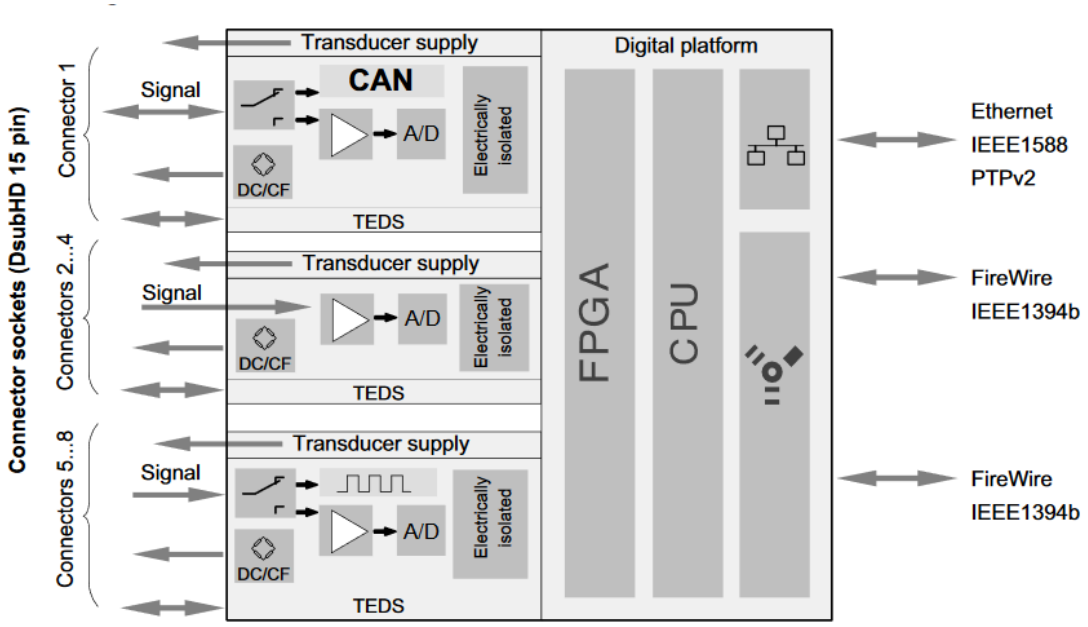

Specification MX840B

General specifications		
Inputs	Number	8, electrically isolated from each other and from the supply voltage[1)]
Transducer technologies		Strain gauge full and half bridge, quarter-bridge with 1-SCM-SG120/350/700/1000, inductive full and half bridge, piezoresistive full bridge, current-fed piezoelectric transducer (IEPE, ICP®), potentiometric transducers, electrical voltage (100 mV, 10 V, 60 V direct, up to 300 V CAT II with 1-SCM-HV), electrical current (20 mA); resistance (e. g. PTC, NTC, KTY); resistance thermometer (Pt100, Pt500, Pt1000); thermocouples (K, N, E, T, S, ...) with cold junction in the plug (1-THERMO-MXBOARD) **Additional support on channel 5-8:** frequency, incremental rotary encoder, speed sensor (rpm), pulse counter, HBM torque, SSI protocol **Additional for channel 1:** CAN bus, receive any signal or send measurement signals
A/D converter		24 Bit Delta Sigma converter
Sample rates (Domain selectable by software, Factory setting is HBM Classic)	S/s	Decimal: 0.1 … 40,000 HBM Classic: 0.1 … 38,400 [5)]
Signal bandbwidth	Hz	7770 (-3dB) with filter Linear phase, 6667 Hz
Active low-pass filter		Bessel, Butterworth, Linear phase, 0.01 … 6667 Hz (-3dB), Filter OFF [6)]
Transducer identification max. distance of the TEDS module	 m	TEDS, IEEE 1451.4 100
Transducer connection		D-SUB-15HD
Supply voltage range (DC)	V	10 ... 30 (24 V nominal (rated) voltage)
Supply voltage interruption		max. 5 ms at 24 V
Power consumption without adjustable transducer excitation with adjustable transducer excitation	 W W	 < 9 < 12
Transducer Excitation (active transducers) Adjustable supply voltage (DC) Maximum output power	 V W	 5 ... 24; adjustable for each channel 0.7 each channel / a total of 2

Ethernet (data link)		10Base-T / 100Base-TX
Protocol/addressing	-	TCP/IP (direct IP address or DHCP)
Connection	-	8P8C plug (RJ-45) with twisted pair cable, Streaming (CAT-5)
Max. cable length to module	m	100
Synchronization		
Firewire		IEEE1394b (2 ports per device)
Ethernet		IEEE1588 (PTPv2) or NTP
EtherCAT®4)		via CX27B EtherCAT Gateway module
IRIG-B		IRIG-B (B000 up to B007; B120 up to B127) via MX440B / MX840B input channel
IEEE1394b FireWire (module synchronization, data link, optional supply voltage)		IEEE 1394b (HBM modules only)
Baud rate	MBaud	400 (approx. 50 MByte/s)
Max. current from module to module	A	1.5
Max. cable length between the nodes	m	5
Max. number of modules connected in series (daisy chain)	-	12 (=11 Hops)
Max. number of modules in a IEEE1394b FireWire system (including hubs2), backplane)	-	24
Max. number of hops3)	-	14
Nominal (rated) temperature range	°C [°F]	-20 ... +65 [-4 ... +149]
Storage temperature range	°C [°F]	-40 ... +75 [-40 ... +167]
Rel. humidity	%	5 ... 95 (non condensing)
Protection class		III
Degree of protection		IP20 per EN 60529 (IP67-version available)
Mechanical tests7)		
Vibration (30 min)	m/s^2	50
Shock (6 ms)	m/s^2	350
EMC requirements		per EN 61326
Max. input voltage at transducer socket to ground		
PIN 1, 2, 3, 4, 5, 7, 8, 10, 13, 15 to Pin 6	V	+ 5.5 (no transients)
PIN 14 (voltage) to Pin 9	V	± 60 (no transients)
Dimensions, horizontal (W x H x D)	mm	52.5 x 200 x 121 (with case protection) 44 x 174 x 116.5 (without case protection)
Weight, approx.	g	980

1) When the variable transducer supply is used, there is no electrical isolation from the supply voltage.

2) Hub: IEEE1394b FireWire node or distributor

3) Hop: Transition from module to module or signal conditioning / distribution via IEEE1394b FireWire (hub, backplane)

4) EtherCAT is a registered trademark and patented technology, licensed by Beckhoff Automation GmbH, Germany.

5) When bridge excitation with carrier frequency (CF) is used, the maximum sample rate is $19.2\frac{kS}{s}$ per channel.

6) Filter OFF is recommended only for real-time applications, e.g. to enable short latency times to be implemented.

7) Mechanical stress is tested according to European Standard EN60068-2-6 for vibrations and EN60068-2-27 for shock.

The equipment is subjected to an acceleration of 50 $\frac{m}{s^2}$ in a frequency range of $5 \div 65Hz$ in all 3 axes. Duration of this vibration test: 30min per axis. The shock test is performed with a nominal acceleration of 350 $\frac{m}{s^2}$ for $6ms$, half sine pulse shape, with 3 shocks in each of the 6 possible directions.

Strain gauge half bridge, 5 or 10 mV/V measuring range, bridge excitation DC voltage		
Accuracy class		0.1
Bridge excitation voltage (effective)	V	1 and 2.5 (±5 %)
Transducers that can be connected		strain gauge half bridges
Permissible cable length between MX840B and transducer	m	< 100
Measuring ranges at 2.5 V excitation at 1 V excitation	 mV/V mV/V	 ±5 ±10
Transducer impedance at 2.5 V excitation at 1 V excitation	 Ω Ω	 300 ... 1,000 80 ... 1,000
Noise at 25 °C and 2.5 V excitation (peak to peak) with filter 1 Hz Bessel with filter 10 Hz Bessel with filter 100 Hz Bessel with filter 1 kHz Bessel	 µV/V µV/V µV/V µV/V	 < 1 < 1.2 < 1.5 < 2
Linearity error	%	< 0.02 of full scale
Zero drift (2.5 V excitation)	% / 10 K	< 0.1 of full scale
Full-scale drift (2.5 V excitation)	% / 10 K	< 0.1 of measurement value
Resistive (strain gauge) full bridge, 100 mV/V measuring range, bridge excitation DC voltage e.g. for piezoresistive transducers		
Accuracy class		0.05
Excitation voltage (DC)	V	2.5 ±5%
Transducers that can be connected		piezoresistive strain gauge full bridges
Permissible cable length between MX840B and transducer	m	< 100
Measuring range	mV/V	±100
Transducer impedance	Ω	300 ... 1,000
Noise at 25 °C (peak to peak) with filter 1 Hz Bessel with filter 10 Hz Bessel with filter 100 Hz Bessel with filter 1 kHz Bessel	 µV/V µV/V µV/V µV/V	 < 3 < 4 < 5 < 10
Linearity error	%	< 0.02 of full scale
Zero drift	% / 10 K	< 0.02 of full scale
Full-scale drift	% / 10 K	< 0.05 of measurement value
Resistive (strain gauge) full bridge, 1000 mV/V measuring range, bridge excitation DC voltage e.g. for piezoresistive transducers		
Accuracy class		0.05
Bridge excitation voltage (DC)	V	2.5 ±5%
Transducers that can be connected		piezoresistive strain gauge full bridges
Permissible cable length between MX840B and transducer	m	< 100
Measuring range	mV/V	±1,000
Transducer impedance	Ω	300 ... 1,000
Noise at 25 °C (peak to peak) with filter 1 Hz Bessel with filter 10 Hz Bessel with filter 100 Hz Bessel with filter 1 kHz Bessel	 µV/V µV/V µV/V µV/V	 < 10 < 20 < 40 < 100
Linearity error	%	< 0.02 of full scale
Zero drift	% / 10 K	< 0.02 of full scale
Full-scale drift	% / 10 K	< 0.05 of measurement value

Inductive full bridge, 100 mV/V measuring range, bridge excitation AC		
Accuracy class		0.05
Carrier frequency (sine)	Hz	4,800 ±1.5
Bridge excitation voltage (effective)	V	1 and 2.5 (±5 %)
Transducers that can be connected		inductive full bridges
Permissible cable length between MX840B and transducer	m	< 100
Measuring ranges at 2.5 V excitation at 1 V excitation	 mV/V mV/V	 ±100 ±300
Signal bandwidth (-3 dB)	kHz	0 ... 1.6
Transducer impedance at 2.5 V excitation at 1 V excitation	 Ω Ω	 300 ... 1,000 80 ... 1,000
Noise at 25 °C and 2.5 V excitation (peak to peak) with filter 1 Hz Bessel with filter 10 Hz Bessel with filter 100 Hz Bessel with filter 1 kHz Bessel	 µV/V µV/V µV/V µV/V	 < 1 < 2 < 5 < 15
Linearity error	%	< 0.02 of full scale
Zero drift (2.5 V excitation)	% / 10 K	< 0.02 of full scale
Full-scale drift (2.5 V excitation)	% / 10 K	< 0.05 of measurement value
Inductive full bridge, 1000 mV/V measuring range, bridge excitation AC		
Accuracy class		0.1
Carrier frequency (sine)	Hz	4800 ±1.5
Bridge excitation voltage (effective)	V	1 (±5 %)
Transducers that can be connected		inductive full bridges
Permissible cable length between MX840B and transducer	m	< 100
Measuring range	mV/V	±1,000
Signal bandwidth (-3 dB)	kHz	0 ... 1.6
Transducer impedance	Ω	80 ... 1000
Noise at 25 °C (peak to peak) with filter 1 Hz Bessel with filter 10 Hz Bessel with filter 100 Hz Bessel with filter 1 kHz Bessel	 µV/V µV/V µV/V µV/V	 < 10 < 30 < 100 < 300
Linearity error	%	< 0.02 of full scale
Zero drift	% / 10 K	< 0.02 of full scale
Full-scale drift	% / 10 K	< 0.1 of measurement value
Inductive half bridge, 100 mV/V measuring range, bridge excitation AC		
Accuracy class		0.1
Carrier frequency (sine)	Hz	4,800 ±1.5
Bridge excitation voltage (effective)	V	1 and 2.5 (±5 %)
Transducers that can be connected		inductive half bridges
Permissible cable length between MX840B and transducer	m	< 100
Measuring ranges at 2.5 V excitation at 1 V excitation	 mV/V mV/V	 ±100 ±300
Signal bandwidth (-3 dB)	kHz	0 ... 1.6
Transducer impedance at 2.5 V excitation at 1 V excitation	 Ω Ω	 300 ... 1,000 80 ... 1,000
Noise at 25 °C and 2.5 V excitation (peak to peak) with filter 1 Hz Bessel with filter 10 Hz Bessel with filter 100 Hz Bessel with filter 1 kHz Bessel	 µV/V µV/V µV/V µV/V	 < 1 < 2 < 5 < 15
Linearity error	%	< 0.02 of full scale
Zero drift (2.5 V excitation)	% / 10 K	< 0.1 of full scale
Full-scale drift (2.5 V excitation)	% / 10 K	< 0.1 of measurement value

LVDT, Linear Variable Differential Transformer (i.e. displacement transducer), AC bridge excitation		
Accuracy class		0.1
Carrier frequency (sine)	Hz	4800±1.5
Bridge excitation voltage (effective)	V	1 (±5 %)
Transducers that can be connected		LVDT
Permissible cable length between MX840B and transducer	m	< 100
Measuring range	mV/V	±3,000
Signal bandwidth (-3 dB)	kHz	0 ... 1.6
Transducer impedance	mH	4 ... 33
Noise at 25 °C (peak to peak) with filter 1 Hz Bessel with filter 10 Hz Bessel with filter 100 Hz Bessel with filter 1 kHz Bessel	 µV/V µV/V µV/V µV/V	 < 10 < 30 < 100 < 300
Linearity error	%	< 0.02 of full scale
Zero drift	% / 10 K	< 0.1 of full scale
Full-scale drift	% / 10 K	< 0.1 of measurement value
Potentiometric transducers / potentiometer		
Accuracy class		0.1
Excitation voltage (DC)	V	2.5 (±5 %)
Transducers that can be connected		potentiometric transducers
Permissible cable length between MX840B and transducer	m	< 100
Measuring range	mV/V	±500
Transducer impedance	Ω	300 ... 5,000
Noise at 25 °C (peak to peak) with filter 1 Hz Bessel with filter 10 Hz Bessel with filter 100 Hz Bessel with filter 1 kHz Bessel	 µV/V µV/V µV/V µV/V	 < 10 < 20 < 40 < 100
Linearity error	%	< 0.02 of full scale
Zero drift (1 V excitation)	% / 10 K	< 0.1 of full scale
Full-scale drift (1 V excitation)	% / 10 K	< 0.1 of measurement value
Current-fed piezoelectric transducers (IEPE - Integrated Electronics Piezo Electric, ICP®)		
Accuracy class		0.1
Transducer technology		IEPE (BNC adapter available: 1-SUBHD15-BNC)
Permissible cable length between MX840B and transducer May be laid inside closed buildings only	m	< 30
Transducer identification (TEDS, IEEE 1451.4)		only version 1.0
Transducer excitation	mA	4,0 ±15%
Measuring ranges (AC)	V	±10
IEPE Compliance Voltage, typ.	V	21
Noise at 25 °C and measuring range ±10 V (peak to peak) at 1 Hz Bessel filter at 10 Hz Bessel filter at 100 Hz Bessel filter at 1 kHz Bessel filter	 µV µV µV µV	 < 200 < 300 < 500 < 1.000
Linearity error	%	< 0.1 of full scale value
Common-mode rejection at DC common-mode at 50 Hz common-mode, typically	 dB dB	 > 100 75
Max. common-mode voltage (to housing and supply ground)	V	±60
Zero drift	% / 10 K	< 0.1 of full scale value
Full-scale drift	% / 10 K	< 0.05 of measurement value

±10 V electrical voltage		
Accuracy class		0.05
Transducers that can be connected		voltage generator up to ±10 V
Permissible cable length between MX840B and transducer	m	BNC adapter available: 1-SUBHD15-BNC < 100
Measuring range	V	±10
Internal resistance of the voltage source	Ω	< 500
Internal impedance, typ.	MΩ	1
Noise at 25 °C (peak to peak) with filter 1 Hz Bessel with filter 10 Hz Bessel with filter 100 Hz Bessel with filter 1 kHz Bessel	 µV µV µV µV	 < 200 < 300 < 500 < 1.000
Linearity error	%	< 0.02 of full scale
Common-mode rejection with DC common mode with 50 Hz common mode, typ.	 dB dB	 > 100 75
Maximum common-mode voltage (to housing and supply ground)	V	±60
Zero drift	% / 10 K	< 0.02 of full scale
Full-scale drift	% / 10 K	< 0.05 of measurement value

0 / 4...20 mA (2, 3, 4-wire) signal current		
Accuracy class		0.05
Transducers that can be connected		transducers with current output (0 ... 20 mA or 4 ... 20 mA)
Permissible cable length between MX840B and transducer	m	< 100
Measuring range	mA	±20
Measurement resistance value, typ.	Ω	10
Noise at 25 °C (peak to peak) with filter 1 Hz Bessel with filter 10 Hz Bessel with filter 100 Hz Bessel with filter 1 kHz Bessel	 µA µA µA µA	 < 1 < 1.5 < 15 < 40
Linearity error	%	< 0.02 of full scale
Common-mode rejection with DC common mode with 50 Hz common mode, typ.	 dB dB	 > 100 75
Maximum common-mode voltage (to housing and supply ground)	V	±30
Zero drift	% / 10 K	< 0.05 of full scale
Full-scale drift	% / 10 K	< 0.05 of measurement value

Ohmic resistance		
Accuracy class		0.1
Transducers that can be connected		PTC, NTC, KTY, TT-3, resistances generally (connection with 4 wire configuration)
Permissible cable length between MX840B and transducer	m	< 100
Measuring ranges	Ω	0 ... 5,000
Excitation current	mA	0.4 ... 0.8
Noise at 25 °C (peak to peak) with filter 1 Hz Bessel with filter 10 Hz Bessel with filter 100 Hz Bessel with filter 1 kHz Bessel	 Ω Ω Ω Ω	 < 0.1 < 0.2 < 0.5 < 1.5
Linearity error	%	<±0.02 of full scale
Zero drift	% / 10K	<0.02 of full scale
Full-scale drift	% / 10 K	<0.1 of measurement value

Resistance thermometer (Pt100, Pt500, Pt1000)		
Accuracy class		0.1
Transducers that can be connected		Pt100, Pt500, Pt1000 (connection with 4 wire configuration)
Permissible cable length between MX840B and transducer	m	< 100
Linearization range	°C [°F]	-200 ... +848 [-328 ... +1558.4]
Noise at 25 °C (peak to peak)		
with filter 1 Hz Bessel	K	< 0.1
with filter 10 Hz Bessel	K	< 0.2
with filter 100 Hz Bessel	K	< 0.5
with filter 1 kHz Bessel	K	< 1.5
Linearity error	K	<±0.3
Zero drift		
with Pt100, Pt500	K / 10 K	<0.2
with Pt1000	K / 10 K	<0.1
Full-scale drift		
with Pt100	K / 10 K	<0.5
with Pt500	K / 10 K	< 0.8
with Pt1000	K / 10 K	< 1

Thermocouples[1)]		
Transducers that can be connected		Thermocouples (type B, C, E, J, K, N, R, S, T)
Permissible cable length between MX840B and transducer	m	< 100
Measuring range	mV	±100
Linearization ranges		
Type B (Pt-30 % Rh and Pt-6 % Rh)	°C [°F]	+100 ... +1,820 [+212 ... +3,308]
Type C (W and W-26 % Re)	°C [°F]	0 ... +2300 [+32 ... +4,172]
Type E (Ni-Cr and Cu-Ni)	°C [°F]	-210 ... +1,200 [-346 ... +2,192]
Type J (Fe and Cu-Ni)	°C [°F]	-270 ... +1,372 [-454 ... +2,501.6]
Type K (Ni-Cr and Ni-Al)	°C [°F]	-270 ... +1,300 [-454 ... +2,372]
Type N (Ni-14,2 % Cr and Ni-4,4 % Si-0,1 % Mg)	°C [°F]	-50 ... +1,768 [-58 ... +3214.4]
Type R (Pt-13 % Rh and Pt)	°C [°F]	-50 ... +1,768 [-58 ... +3214.4]
Type S (Pt-10 % Rh and Pt)	°C [°F]	-270 ... +400 [-454 ... +752]
Type T (Cu and Cu-Ni)		
Transducer impedance	Ω	< 500
Noise Type K (peak to peak)		
with Filter 1 Hz Bessel	K	0.05
with Filter 10 Hz Bessel	K	0.1
with Filter 100 Hz Bessel	K	0.5
with Filter 1 kHz Bessel	K	1
Total error limit at 22 °C ambient temperature		
Type E, J, K, T, C	K	±1.5
Type R, S	K	±4
Type B	K	±15
Temperature drift (type K)	K / 10K	<±0.5
Cold junction 1-THERMO-MXBOARD		
Nominal (rated) temperature range	°C [°F]	-20 ... +60 [-4 ... +140]
Operating temperature range	°C [°F]	-20 ... +65 [-4 ... +149]
Storage temperature range	°C [°F]	-40 ... +75 [-40 ... +167]

1) One of the following cold junctions is required for connecting thermocouples to the MX840B (ordering no.: 1-THERMO-MXBOARD; 1-SCM-TCK; 1-SCM-TCE; 1-SCM-TCJ; 1-SCM-TCT)

Digital control output (e.g. for triggering of external shunts, reset of external charge amplifiers)		
Output type		High side switch
Reference potential		Pin 6 (ground)
High level		
Output unloaded, typ.	V	5
I_{out} = 5 mA	V	> 4.5
Permissible load impedance	kΩ	> 1

Frequency or pulse counting (connections 5 ... 8)		
Accuracy class		0.01
Transducers that can be connected		in general timer-based digital signal sources (single lane, dual lane, with/without index), pulse counter, incremental rotary encoder, HBM-torque transducer (digital), SSI transducers (absolute position)
Permissible cable length between MX840B and transducer	m	< 50
Signals F_1 (±) F_2 (±) Zero index (±)		 Frequency or pulse signal Direction of rotation signal shifted by ±90° to F_1 or static Zero position signal
Input level with differential operation Low level High level		 Differential inputs (RS422): Signal (+) < Signal (-) -200 mV Differential inputs (RS422): Signal (+) > Signal (-) +200 mV
Input level with unipolar operation Low level High level	 V V	 <1.5 > 3.5
Maximum input voltage at transducer socket to ground (pin 6)	V	5.5 (no transients)
Measuring ranges Frequency Pulse counting	 Hz pulses/s	 0.1 ... 1,000,000 0 ... 1,000,000
Input impedance, typ.	kΩ	10
Temperature drift	% / 10 K	< 0,01 of measurement value
SSI mode (differentially) Shift clock Word length Code Input level Low level High level Signals Data Shift clock	 kHz Bit 	 100, 200, 500, 1,000 12-31 binary or gray Differential inputs (RS422): Signal (+) < Signal (-) -200 mV Differential inputs (RS422): Signal (+) > Signal (-) +200 mV Data+, Data- (RS-422) Clk+, Clk- (RS-422)

CAN (connection 1)									
Supported protocols		CAN 2.0A, CAN 2.0B							
Number of CAN ports		only connector 1							
Bus link		two wire, according to ISO11898							
Bit rates	KBit / s	1000	800	666,6	500	400	250	125	100
Permissible cable lengths	m	25	50	80	100	100	250	500	500
Bit sequence		Intel standard, Motorola forward MSB							
Receiving[1)], can be parameterized via CANdb *.dbc Rate in total Number of CAN signals CAN signal types	1/s	 max. 10,000 ≤ 128 standard, mode-dependent, mode-Signal							
Transmitting, MX Assistant generates CANdb (*.dbc) Transmission rate per signal (max.) Number of analog input signals (modul-internal only) Generate dbc file (Assistant)	1/s	 100 per signal 7 with MX Assistant							

1) Parameterization from CANdb via catmanEASY or MX Assistant

Decimal sample rates and digital low pass filter, type Bessel 4^{th} order

Type	-1dB (Hz)	-3dB (Hz)	-20dB (Hz)	Phase delay*) (ms)	Rise time (ms)	Overshoot (%)	Sample rate (Hz)
Bessel	3,041	5,000	9,935	0.043	0.08	3.6	40,000
	1,188	2,000	5,141	0.13	0.2	0.9	40,000
	594	1,000	2,561	0.29	0.3	0.85	40,000
	296	500	1273	0.62	0.7	0.8	40,000
	118	200	508	1.6	1.7	0.8	40,000
	59	100	254	3.2	3.5	0.8	40,000
	30	50	127	6.5	7	0.8	40,000
	12	20	51	16.4	17.5	0.8	40,000
	6	10	25	34.5	35	0.8	20,000
	3	5	13	69	70	0.8	10,000
	1.2	2	5.1	168	175	0.8	10,000
	0.6	1	2.5	332	350	0.8	5000
	0.3	0.5	1.3	663	700	0.8	1000
	0.1	0.2	0.5	1652	1750	0.8	1000
	0.06	0.1	0.25	3299	3500	0.8	500
	0.03	0.05	0.13	6598	7003	0,8	100
	0.01	0.02	0.05	16,495	17,508	0,8	100
	0.006	0.01	0.02	32,989	35,016	0,8	50

Decimal sample rates: Amplitude response Bessel filter

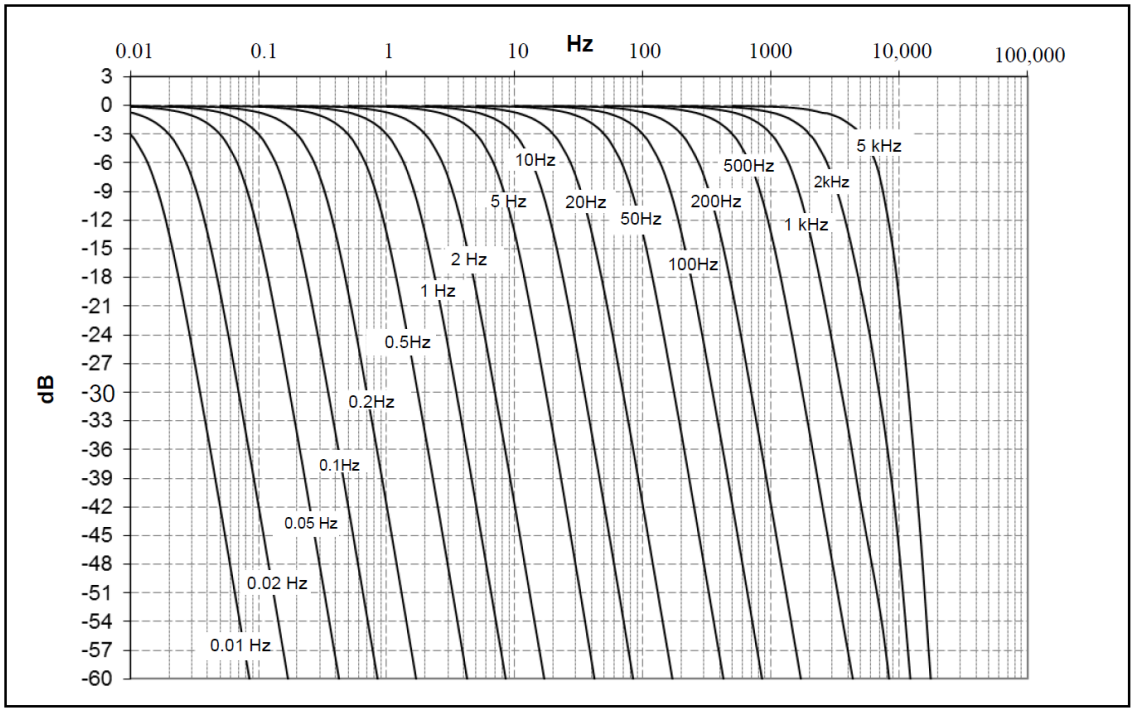

Decimal sample rates and digital low pass filter, type Butterworth 4^{th} order

Type	-1dB (Hz)	-3dB (Hz)	-20dB (Hz)	Phase delay*) (ms)	Rise time (ms)	Overshoot (%)	Sample rate (Hz)
Butterworth	5,198	6,090	8,722	0.08	0.08	15.2	40,000
	4,274	5,000	7,667	0.10	0.09	13.7	40,000
	1,690	2,000	3,491	0.23	0.2	11	40,000
	844	1,000	1,768	0.46	0.4	10.9	40,000
	422	500	888	0.9	0.8	10.8	40,000
	169	200	355	2.2	1.9	10.8	40,000
	84	100	178	4.5	3.9	10.8	40,000
	42	50	89	9.2	7.7	10.8	20,000
	17	20	35.5	23	19.3	10.8	20,000
	8.4	10	17.8	45	39	10.8	20,000
	4	5	8.9	90	77	10.8	20,000
	1.7	2	3.5	225	193	10.9	20,000
	0.8	1	1.8	449	387	10.8	20,000
	0.4	0.5	0.9	898	774	10.8	10,000
	0.17	0.2	0.3	2241	1930	10.9	10,000
	0.08	0.1	0.18	4481	3861	10.9	5000
	0.04	0.05	0.09	8962	7721	10.9	1000
	0.02	0.02	0.03	22,405	19,303	10.9	1000
	0.008	0.01	0.02	44,810	38,606	10.9	500

*)The delay time of the ADC is 65 μs for the sample rate 38,400 Hz and 128 μs for the all other sample rates. This value has not been accounted in the "phase delay" column above.

Decimal sample rates: Amplitude response Butterworth filter

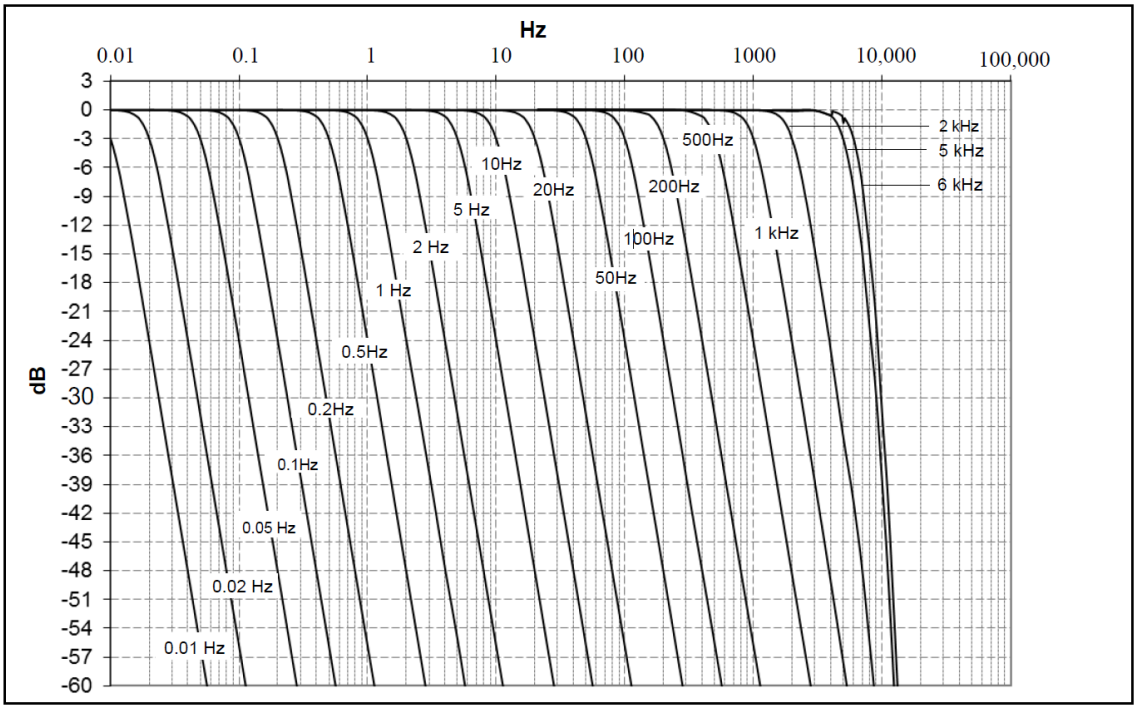

Decimal sample rates and digital low-pass filters, linear phase (FIR)

Type	Start of level drop (Hz)	-3 dB (Hz)	-20 dB (Hz)	Runtime*) (ms)	Rise time (ms)	Overshoot (%)	Sample rate (Hz)
Linear Phase	6,667	7,770	9,220	0.41	0.06	8.6	40,000
	3,333	3,800	4,540	0.78	0.12	8.6	40,000
	1,667	2,120	2,700	2.41	0.28	8.6	5,000
	1,000	1,130	1,300	6.21	0.544	8.6	2,500
	833	1,050	1,345	4.01	0.551	8.6	2,500
	667	840	1,080	4.8	0.694	8.6	1,000
	333	420	540	10.4	1.39	8.6	1,000
	167	210	270	26.9	2.73	8.6	500
	67	84	108	50.2	6.88	8.6	200
	33	42	54	108	13.8	8.6	100

*)The A/D converter's delay time for all sample rates is 65 μs and this is not taken into account in the "runtime" column!

Decimal sample rates: amplitude response, linear phase (FIR)

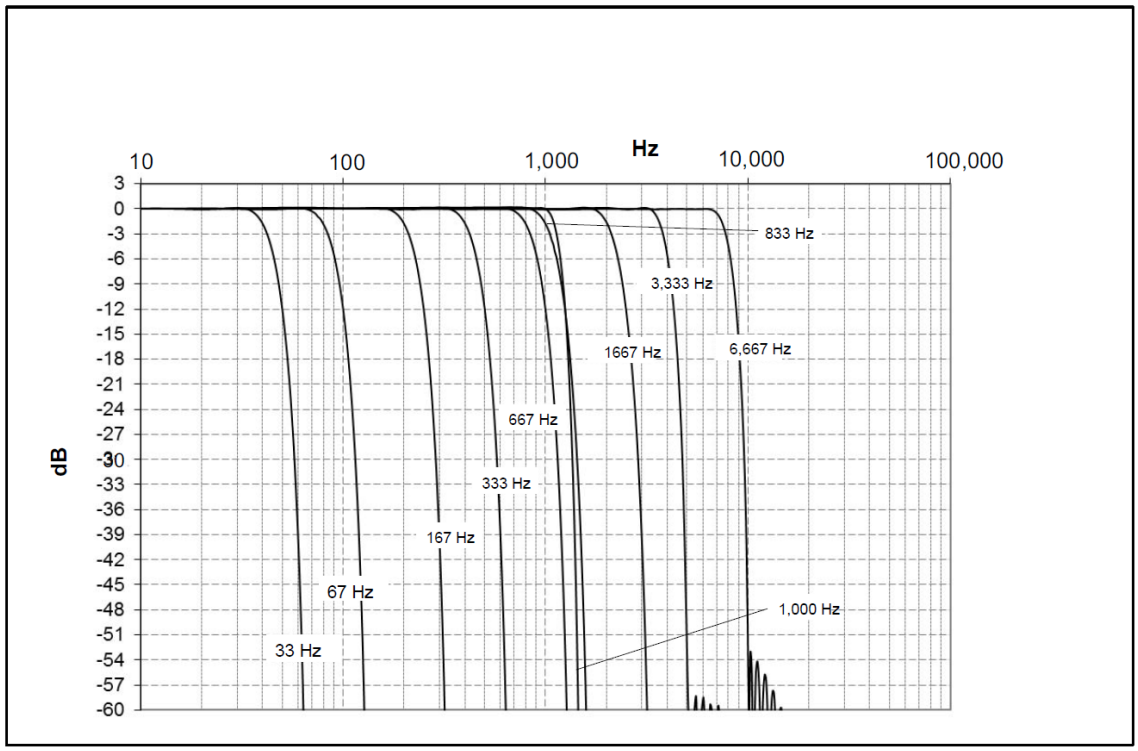

Decimal sample rates and digital low-pass filters, Butterworth (FIR)

Type	Start of level drop (Hz)	-3 dB (Hz)	-20 dB (Hz)	Runtime*) (ms)	Rise time (ms)	Overshoot (%)	Sample rate (Hz)
Butterworth	1,498	1,700	2,220	3.2	0.285	15.6	10,000
	1,384	1,500	1,887	3.48	0.346	18.7	10,000
	698	750	924	5.56	0.682	18.7	5,000
	344	370	471	14.1	1.40	18.7	2,500
	275	300	377	17.3	1.75	18.7	1,000
	140	150	185	27.6	3.41	18.7	1,000
	69	75	94	71.8	6.97	18.7	500
	28	30	37	139	17.0	18.7	200
	14	15	19	358	34.9	18.7	100

The A/D converter's delay time for all sample rates is 65 μs and this is not taken into account in the "runtime" column!

Decimal sample rates: Butterworth filter amplitude response (FIR)

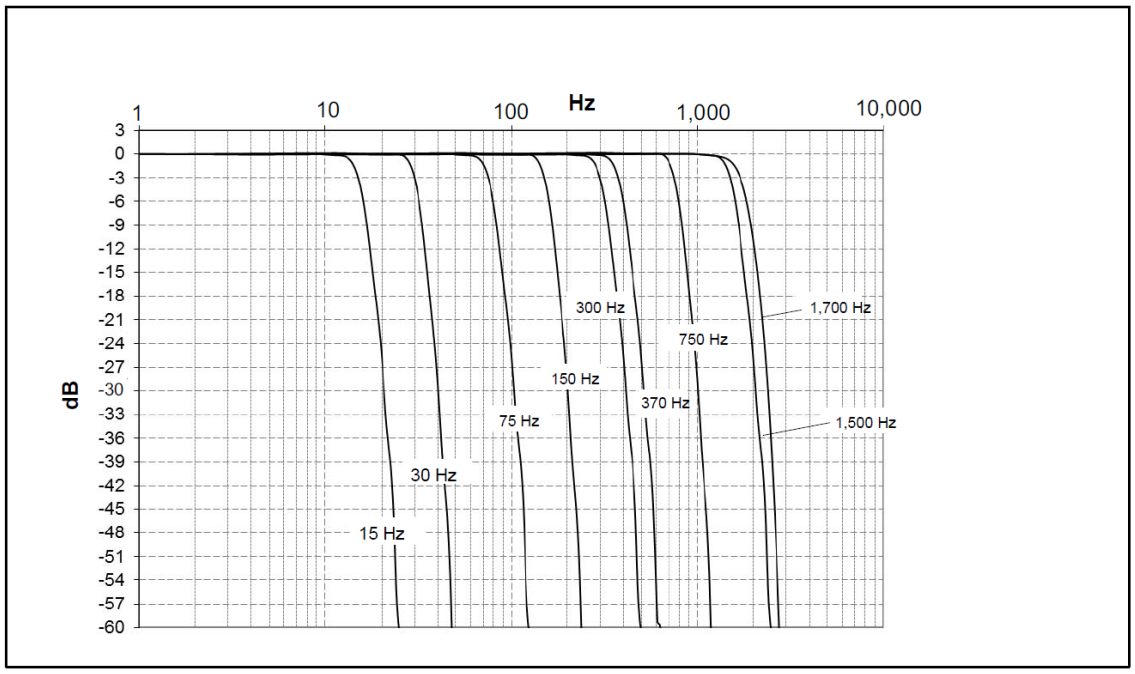

Classic HBM sample rates and digital low pass filter, type Bessel 4^{th} order

Type	-1dB (Hz)	-3dB (Hz)	-20dB (Hz)	Phase delay (ms)*)	Rise time (ms)	Overshoot (%)	Sample rate (Hz)
Bessel	3000	5161	13,086	0.012	0.07	0.157	38,400
	2000	3210	8100	0.15	0.1	1.5	19,200
	1000	1630	4050	0.24	0.2	1.4	19,200
	1000	1640	5150	0.21	0.2	0.7	9600
	500	820	2120	0.4	0.43	1.4	9600
	200	335	860	1	1.04	1	9600
	100	167	430	2	2.1	0.8	9600
	50	83	215	4	4.28	0.8	9600
	20	33.7	85	10	10.6	0.8	9600
	10	16.5	42	20	21.3	0.8	9600
	5	8.4	21	40	41.6	0.8	2400
	2	3.4	8.5	99	104	0.8	2400
	1	1.6	4.2	200	214	0.8	2400
	0.5	0.83	2.1	400	420	0.8	300
	0.2	0.34	0.85	1000	1060	0.8	300
	0.1	0.17	0.43	2000	2130	0.8	300
	0.05	0.084	0.21	3940	4200	0.8	20
	0.02	0.033	0.085	10,000	10,600	0.8	20
	0.01	0.017	0.042	20,100	21,300	0.8	20

The delay time of the ADC is 65 μs for the sample rate 38,400 Hz and 128 μs for the all other sample rates. This value has not been accounted in the "phase delay" column above.

Classic HBM sample rates : Amplitude response Bessel filter

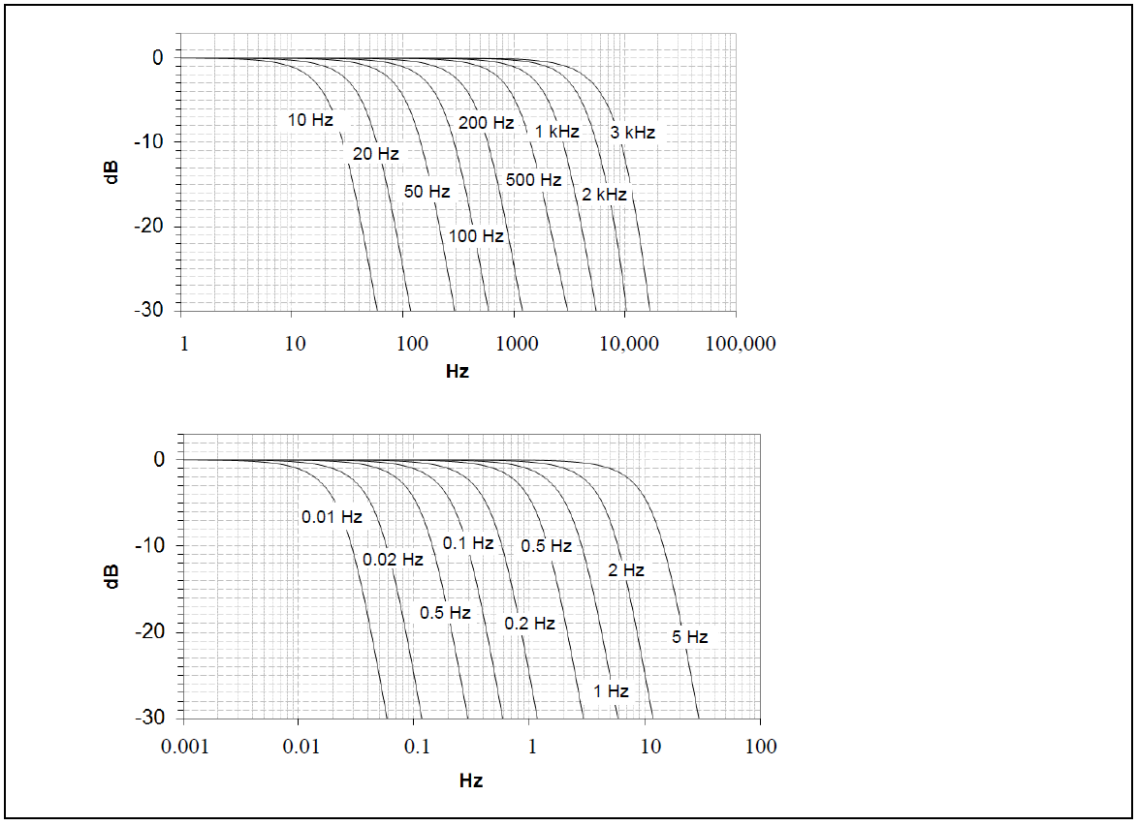

Classic HBM sample rates and digital low pass filter, type Butterworth 4^{th} order

Type	-1dB (Hz)	-3dB (Hz)	-20dB (Hz)	Phase delay (ms)*)	Rise time (ms)	Overshoot (%)	Sample rate (Hz)
Butterworth	6000	6868	9433	0.07	0.07	15.90	38,400
	4000	4660	7324	0.10	0.09	13.52	38,400
	2000	2360	4331	0.2	0.15	8.5	19,200
	1000	1178	2100	0.38	0.3	11	19,200
	1000	1168	2140	0.32	0.32	11	9600
	500	586	1050	0.66	0.66	11	9600
	200	235	420	1.7	1.6	11	9600
	100	118	210	3.46	3.2	11	9600
	50	59	105	6.98	6.6	11	9600
	20	24	42	17.3	16	11	9600
	10	12	21	34.9	32	11	9600
	5	5.95	10.5	69	66	11	2400
	2	2.37	4.24	173	160	11	2400
	1	1.26	2.1	347	320	11	2400
	0.5	0.59	1.05	701	660	11	300
	0.2	0.236	0.421	1760	1600	11	300
	0.1	0.118	0.21	3510	3200	11	300
	0.05	0.059	0.105	6950	6600	11	20
	0.02	0.0235	0.042	17,500	16,000	11	20
	0.01	0.012	0.021	34,600	32,000	11	20

The delay time of the ADC is 65 μs for the sample rate 38,400 Hz and 128 μs for the all other sample rates. This value has not been accounted in the "phase delay" column above.

Classic HBM sample rates : Amplitude response Butterworth filter

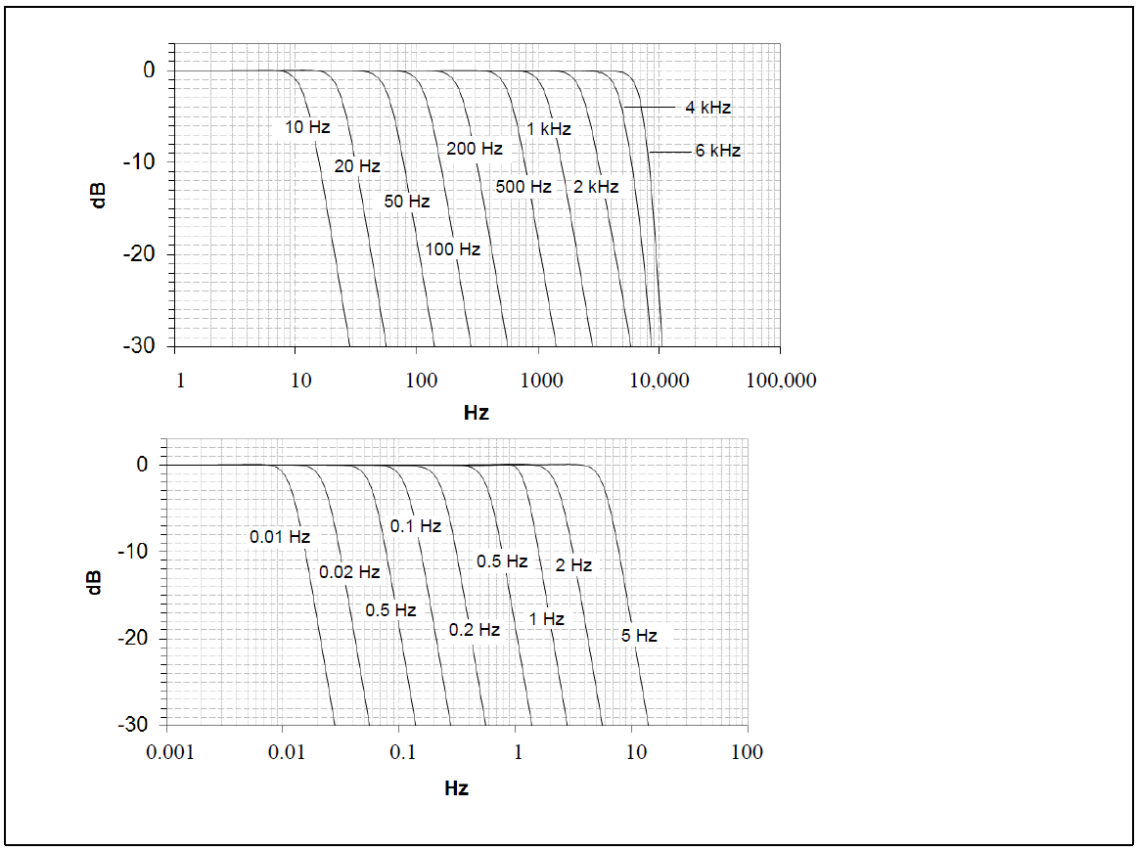

Digital Charge Amplifier

A charge amplifier is an electronic current integrator that produces a voltage output proportional to the integrated value of the input current, or the total charge injected.
The amplifier offsets the input current using a feedback reference capacitor, and produces an output voltage inversely proportional to the value of the reference capacitor but proportional to the total input charge flowing during the specified time period. The circuit therefore acts as a charge-to-voltage converter. The gain of the circuit depends on the values of the feedback capacitor.

CMD 600

Special feature:

- Digital charge amplifier for piezoelectricsensors
- Two separate parameter sets(measurement programs)
- Measuring range adjustable as requiredor via SensorTeach
- TEDS sensor detection
- Signal output $\pm$ 10V
- Fast and configurable digitalinputs/outputs
- All signal inputs and outputs electricallyisolated
- Ethernet system interface
- Compact, robust design, IP60
- IP65 version (CMD600-P)
- User-friendly parameterization software, LabView drivers and Siemens S7 operation blocks

Block Diagram

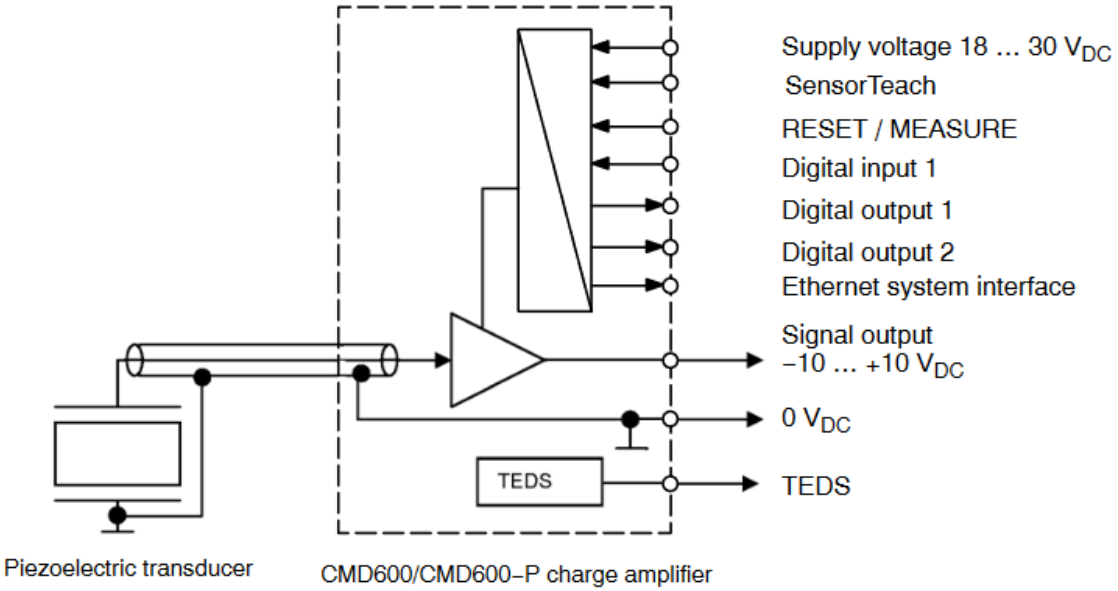

Specification

Charge amplifier		**CMD600/CMD600−P**
Transducers that can be connected		Piezoelectric sensors
Charge inputs		1
Measuring range adjustable as required or via SensorTeach for fast teach-in processes	pC	±50 … ±600 000
Calibrated measuring ranges	% F_{nom}	100
Signal output, analog		
Output voltage	V	−10 …+10
Signal source		current measured value, min./max. value, peak-to-peak value
Output voltage limiting	V	±11
Output current, max., short-circuit proof	mA	10
Output resistance	Ω	< 5
Interference suppression between input and output (GND) (0 … 1000 Hz)	dB	> 60
Output interference signal (0.1 Hz … 1 MHz, peak-to-peak) over the full measuring range ±50 … ±600000 pC up to 30 kHz filter frequency	mV	< 30
Time from switch-on to stable output values	ms	375
TEDS as per IEEE1451.4		1-wire
Measurement accuracy		
Accuracy class (at 25°C)	%	< ±0.5
Repeat accuracy (at 25°C)	%FS	< ±0.05
Reset/Measure (operate) step	pC	< ±2 (typ. < 1)
Drift (at 20°C)	pC/s	< ±0.05

Analog signal output frequency response		
Measurement frequency range (–3 dB)		
Measuring range 50 pC to 32 000 pC	kHz	30
Measuring range 32 000 pC to 40 000 pC	kHz	24
Measuring range 40 000 pC to 60 000 pC	kHz	16
Measuring range 60 000 pC to 80 000 pC	kHz	12
Measuring range 80 000 pC to 100 000 pC	kHz	9.6
Measuring range 100 000 pC to 120 000 pC	kHz	8
Measuring range 120 000 pC to 180 000 pC	kHz	5.3
Measuring range 180 000 pC to 250 000 pC	kHz	3.8
Measuring range 250 000 pC to 400 000 pC	kHz	2.4
Measuring range 400 000 pC to 600 000 pC	kHz	1.6
Low-pass filter, selectable up to 20 kHz	Hz	1 … 20 000; 30 000
Runtime at 30 kHz cut-off frequency	µs	8.2
Runtime at 20 kHz cut-off frequency	µs	28
Runtime at 10 kHz cut-off frequency	µs	46
Runtime at 1 kHz cut-off frequency	µs	400
Runtime at 100 Hz cut-off frequency	ms	4
Runtime at 10 Hz cut-off frequency	ms	40
Filter characteristics		Fifth-order Bessel
High-pass filter, selectable	Hz	0.15; 1.5; Off
Offset		
Output voltage offset for current measurement signal	V	±10
Resolution	mV	10
Signal output, digital		
Resolution	Bit	14
Accuracy	%FS	< ±1
Sampling rate for peak value acquisition	kHz	10
Control signals (electrically isolated)		
Input voltage range		
High	V	12 … 30
Low	V	0 … 5 or open input
Input current	mA	4, at 24 V Supply
Reset time (5 x RC)		
Measuring range < 6000 pC	ms	3
Measuring range > 6000 pC (adaptive reset from firmware 3.61)		
Output voltage		
> 2V	ms	80
1 … 2 V	ms	60
0.1 … 1 V	ms	40
50 mV … 0.1 V	ms	20
0 … 50 mV	ms	13
Peak-value memories		
Number		3
Function		Min., max., peak-to-peak value
Update rate	ms	0.1
Peak-value memory clearing	ms	2
Limit value switches		
Number		2
Functions		Switching threshold, hysteresis (2-point control)
Signal source		Current measured value
Hysteresis		Adjustable as required
Update	ms	0.1

LED displays		
IP address not configured		Flashing green-blue
Connection via Ethernet		Constant blue
Measure		Constant green
Reset		Constant red
Overload		Flashing red-blue or red-green
SensorTeach function in the 600 000 pC range		Flashing yellow, 1 Hz
SensorTeach function in the 6000 pC range		Flashing yellow, 2 Hz
Ready for firmware update		Flashing white, 2 Hz
Bootloader mode		Flashing red, 1 Hz
Device identification		Blue, yellow, red and green in succession, 2 Hz
Unit connections		
System input/output		M12 plug, pin-compatible with CMA amplifier, 8 pins
Ethernet input		M12 socket, 4 pins, with protective cap
Digital input/output		M12 plug, 5 pins, with protective cap
Sensor input		CMD600: BNC socket; CMD600–P: 10–32 UNF, socket, tightening torque ⩽ 1.5 Nm
Ethernet communications interface		
System interface for amplifier parameterization and transmission of measured values at max. 1 kHz transfer rate		
Transmission protocol	Mbit/s	TCP/IP, can be networked per IEEE802
Transfer rate, max.	Mbit/s	10
Topology (twisted pairs)		2
Connector socket		M12, socket with protective cap
Cable type		UTP category 5 or shielded twisted pair (STP)
Digital control signals		
System input/output		Voltage supply; Reset/Measure; SensorTeach; TEDS; analog output signal
Ethernet input		PC/PLC connection, measured value streaming
Digital input		
Number		1
Switching actions, selectable		One-off, peak-value memory clearing (min./max.), RUN/HOLD analog output signal hold
Response time	ms	0.1
Input voltage range	V	0 … 30
Active input level can also be selected inverted	V	0 or 24
Switching voltages		
Logical High level	V	12 … 30
Logical Low level	V	0 … 5 or open input
Input current at 24 V, typical	mA	4
One-way fitting	V	–30 … 0
Digital input latency times	ms	2
Digital output		
Number		2
Switching actions, selectable		Limit value switch 1 or 2, overload, manual actuation, device error, parameter set selection
Response times	ms	0.1
Active voltage level can also be selected inverted, separately for each output	V	0 or 24
Output voltage (like supply voltage), nom.	V	24
Voltage drop with load, max.	V	1
Output current at operating temperature	mA	350
Short-circuit current, typical	A	0.7
Short-circuit period		unlimited
Latency times of digital outputs	ms	2

General data		
Supply voltage overvoltage and one-way fitting	V_{DC}	24 (18 … 30)
Voltage supply buffer capacitor	µF	220
Electrical isolation		Electrical isolation of signal input and signal output from the voltage supply. Electrical isolation of signal input/signal output from the digital I/Os including the control inputs (Reset/Operate, SensorTeach). No electrical isolation of the digital I/Os and control inputs (Reset/operate, SensorTeach) from the voltage supply. The CMD600 housing must be grounded.
Supply current (24 V), without digital outputs	mA	160
Number of parameter sets/measurement programs in the device		2 plus factory settings, saved in EEPROM
Typical switching times between parameter sets, in the measuring range < 6000 pC without range selection in all other cases	 ms ms	 5 160
Vibration resistance 20 … 2000 Hz, duration 16 min., cycle 2 min. **Impact;** duration 1 ms	 m/s^2 m/s^2	 100 2000
Nominal (rated) temperature range, non-condensing	°C	0 … 60
Operating temperature range, non-condensing	°C	–40 … +80
Relative humidity (maximum), non-condensing	%	93, at +40°C ± 2°C
Dimensions (L x W x H)	mm	115 x 64 x 35
Weight	g	350
Housing material		Die-cast aluminum
Degree of protection, with connected cable or with protective caps		CMD600: IP60; CMD600–P: IP65
EMC conformity		
in accordance with EN 61326–1: 2007, EN 61326–2–3: 2007		in an industrial environment

Connector Pin Assignment

System Input/Output connector Plug (view of pins in CMD600)

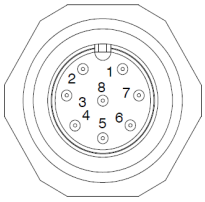

PIN no.	Signal name	Description	Values	Color code KAB 168...
1	Supply ground	–	–	wh
2	SensorTeach	Digital input, active High	+12 … +30 V	br
3	RESET/MEASURE	Digital input, active High	+12 … +30 V	gn
4	TEDS	–	–	ye
5	Charge out	Output signal	±10 V	gy
6	Ground output	Ground output signal	–	pk
7	no function	no function	–	bu
8	Voltage supply	Voltage supply between pins 8 and 1	+18 … +30 V	rd

Ethernet connector socket (view of pins in CMD600)

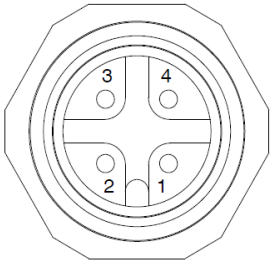

PIN no.	Signal name
1	TX +
2	RX +
3	TX –
4	RX –

CMD600 Ethernet cable pin assignment to PC

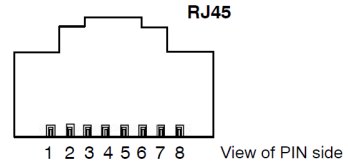

Patch cable

RJ45	M12
1	1
2	3
3	2
6	4

Crossover cable (1-KAB284-2)

RJ45	M12
1	2
2	4
3	1
6	3

Digital I/O connector socket (digital input/outputs, view of pins in CMD600)

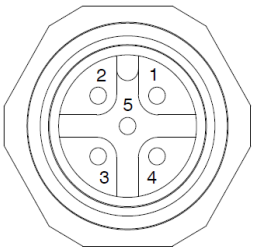

PIN no.	Signal name	Description	Values
1	Digital Out	Digital output 1	VCC/ 350 mA max.
2	VCC	Supply for digital output 1/2	+18 … +30 V
3	Digital Out	Digital output 2	VCC/ 350 mA max.
4	Digital In	Digital input 1	+12 … +30 V
5	Supply ground	–	–

Dimension

Dimensions in mm (1 mm = 0.03937 inches)

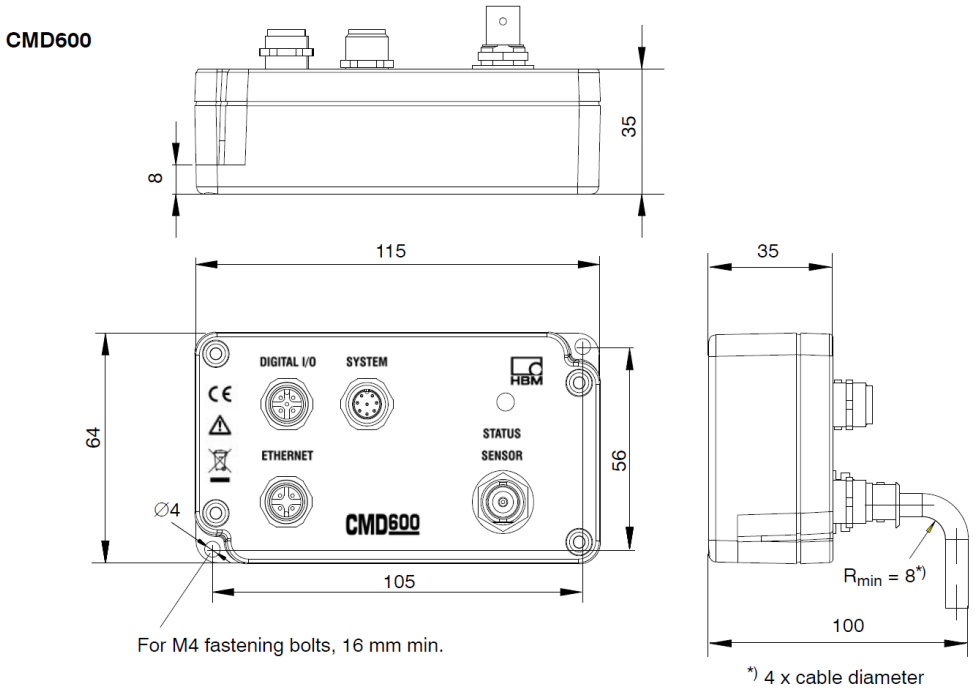

Load Cell

A load cell is a force transducer. It converts a force such as tension, compression, pressure, or torque into an electrical signal that can be measured and standardized. As the force applied to the load cell increases, the electrical signal changes proportionally.
In our scenario, we had to evaluate the normal force and also the shear force. For this reason we choose the CLP 62KN for the normal one and the 4.5KN for the shear one.

CLP 62 KN

Dimension

Dimensions (in mm; 1 mm = 0.03937 inches)

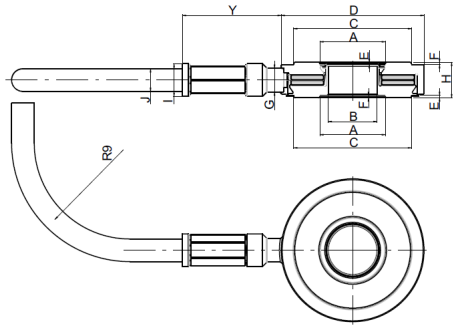

Type	A	B	C	D	E	F	G	H	I	J	Y
CLP/3kN	4.05	2.7^{H7}	6.5	$8^{-0.05}$	0.12	0.15	2	$3^{-0.05}$	~2.7	1.9	~8.3
CLP/7kN	5.5	4.1^{H7}	9.9	$12^{\pm 0.05}$	0.2	0.2	2	$3^{-0.05}$	~2.7	1.9	~8.3
CLP/14kN	7.8	6.1^{H7}	13.9	$16^{-0.05}$	0.29	0.32	2	$3.5^{-0.05}$	~2.7	1.9	~8.3
CLP/26kN	9.8	8.1^{H7}	17.9	$20^{-0.05}$	0.3	0.32	2	$3.5^{-0.05}$	~2.7	1.9	~8.3
CLP/36kN	11.8	10.1^{H7}	21.9	$24^{-0.05}$	0.29	0.32	2	$3.5^{-0.05}$	~2.7	1.9	~8.3
CLP/62kN	13.8	12.1^{H7}	27.9	$30^{-0.05}$	0.5	0.45	2	$4^{-0.05}$	~2.7	1.9	~8.3
CLP/80kN	15.8	14.1^{H7}	33.9	$36^{-0.05}$	0.52	0.52	2	$5^{-0.05}$	~2.7	1.9	~8.3

Specification

Type			CLP/...						
Nominal (rated) force	F_{nom}	kN	**3**	**7**	**14**	**26**	**36**	**62**	**80**
Accuracy									
Relative reversibility error	v	%	1						
Relative linearity error [4]	d_{lin}	%	1						
Electrical characteristics									
Sensitivity (typical) [1]	S	pC/N	-4.3						
Insulation resistance	R_{is}	Ω	> 10^{13}						
Temperature									
Nominal (rated) temperature range	$B_{T,\,nom}$	°C	-20 … +120						
Operating temperature range	$B_{T,\,G}$		-20 … +120						
Storage temperature range	$B_{T,\,S}$		-20 … +120						
Characteristic mechanical qualities									
Max. operating force	F_G	%	115						
Limit force	F_L		150						
Breaking force	F_B		200						
Maximum bending moment with [2] with F_z = 0% of F_{nom} with F_z = 50% of F_{nom} with F_z = 100% of F_{nom}	$M_{b\,perm}$	Nm	0 1.5 0	0 5 0	0 15 0	0 35 0	0 65 0	0 134 0	0 244 0
Static lateral limit force at an initial stress of at least 10% of F_{nom} [3]	F_Q	% of F_{nom}	10						
Nominal (rated) displacement	s_{nom}	µm	3	3	3.5	3.5	4	4	4.5
Fundamental resonance frequency	f_G	kHz	105		120			140	120
Relative permissible oscillatory stress	F_{rb}	% of F_{nom}	100						
General information									
Degree of protection per DIN 60529			IP65						
Sensor material			Stainless steel, quartz						
Cable sheath material			FPM (fluorinated rubber)						
Cable length		m	0.5 or 1						
Connector			10-32UNF						
Ground	m	g	4	5	6	6	10	15	29

1) must be calibrated under mounting condition
2) F_z is the force in the measurement direction
3) Related to a point of contact on the force application surface
4) Under initial stress of at least 20%

CSW 4.5 KN

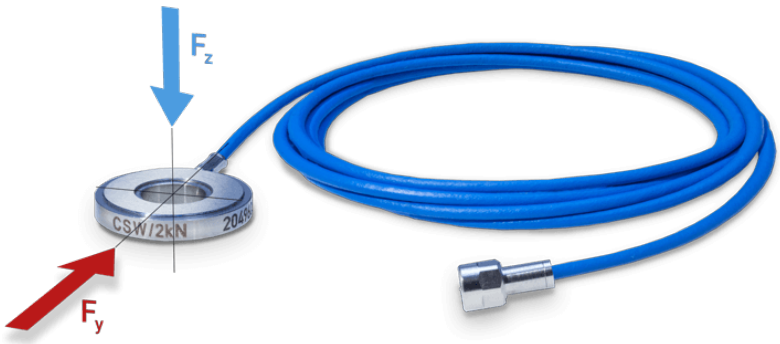

Dimension

Dimensions (in mm; 1 mm = 0.03937 inches)

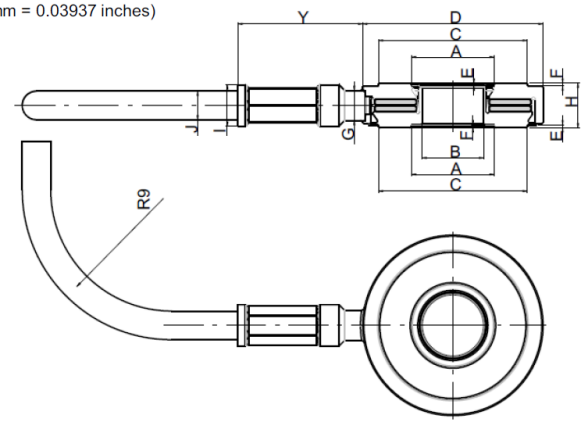

Type	A	B	C	D	R	F	G	H	I	J	Y
CSW/1KN	7.8	6.1 H7	13.9	$16_{-0.05}$	0.29	0.32	2	$3.5_{-0.05}$	~2.7	1.9	~8.3
CSW/2KN	9.8	8.1 H7	17.9	$20_{-0.05}$	0.3	0.32	2	$3.5_{-0.05}$	~2.7	1.9	~8.3
CSW/3KN	11.8	10.1 H7	21.9	$24_{-0.05}$	0.29	0.32	2	$3.5_{-0.05}$	~2.7	1.9	~8.3
CSW/4.5KN	13.8	12.1 H7	27.9	$30_{-0.05}$	0.5	0.32	2	$4_{-0.05}$	~2.7	1.9	~8.3
CSW/8KN	15.8	14.1 H7	33.9	$36_{-0/05}$	0.52	0.32	2	$5_{+0.15/-0.05}$	~2.7	1.9	~8.3

Specification

Nominal (rated) force	**F_{nom}**	**kN**	**1**	**2**	**3**	**4.5**	**8**
Accuracy							
Relative reversibility error	v	%	1				
Non-linearity	d lin	%	1				
Crosstalk from F_z (force in prestressing direction) on the measurement result, typically		%	0.1				
Crosstalk from bending moments M_b on the measurement result, typically		N/Nm	0.6				
Transverse sensitivity (crosstalk from forces transverse to the measurement direction), typically		%	3	2	2	1	1
Rated electrical output							
Sensitivity, typically [1)]	S	pC/N	-7.0	-7.5	-7.5	-7.5	-8.0
Insulation resistance	R_{is}	Ω	$>10^{13}$				
Temperature							
Nominal (rated) temperature range	$B_{t,nom}$	°C	-20…+120				
Operating temperature range	$B_{t,g}$	°C	-20…+120				
Storage temperature range	$B_{t,S}$	°C	-20…+120				
Characteristic mechanical quantities							
Maximum operating force	F_G	% of F_{nom}	110				
Force limit	F_L	% of F_{nom}	125				
Breaking force	F_B	% of F_{nom}	150				
Max. bending moment at [2)]							
With pre-stressing force 500 % of F_{nom}	$M_{B,\ perm}$	Nm	10.2	24	30.5	96.5	100
With pre-stressing force 1000 % of F_{nom}		Nm	1	2.4	3	9.6	10
Maximum pre-stressing force	F_Q	% of F_{nom}	1000				
Nominal (rated) displacement	S_{nom}	µm	3.5	3.5	4	4	4.5
Fundamental frequency	f_G	kHz	120	120	120	140	120
Relative permissible oscillatory stress	F_{rb}	% of F_{nom}	100				
General information							
Degree of protection per EN 60529			IP65				
Sensor material			Stainless steel, quartz				
Cable sheath material			FPM (fluorinated rubber)				
Cable length	L	m	1				
Plug			10-32UNF				
Weight (without cable)	m	g	6	6	10	15	29

Chapter 4

Results

In this chapter will be illustrated all the result obtained from the Motion Analysis using the software "Solidworks" and plotted using the software Matlab.

Stress and Strain Distribution

To Analyze the result I choose the max stress for all the simulation and on the figure below it can ben seen how the stress and strain distributes on the lower arm.

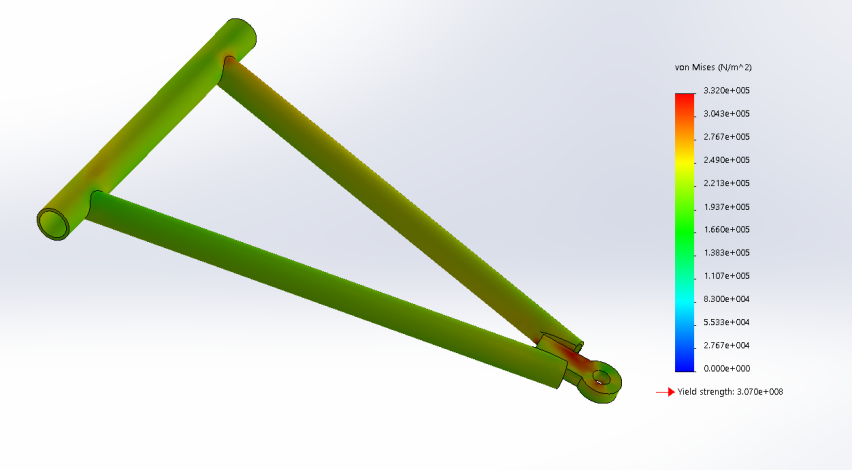

Stress history - Type C Road

When the load applied to the tyre is a the road generated following the ISO standard the max stress generated on the lower control arm follows this behavior.

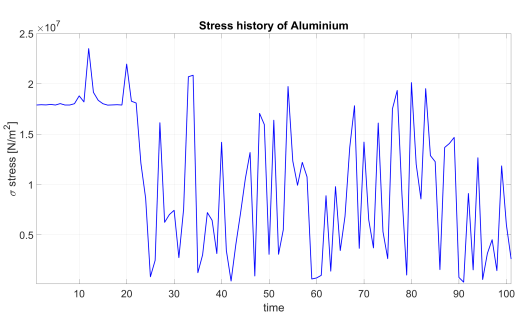

This one is when the material chosen is Aluminium.

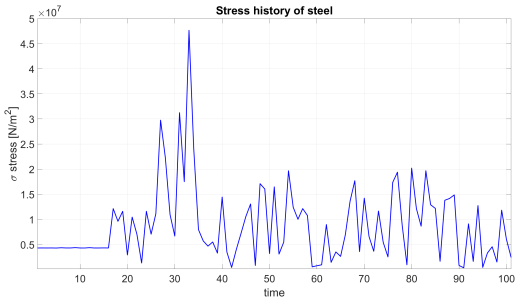

This on instead is the behavior if the material is Steel.

Stress History - Type C

The strain follows this behaviour instead:

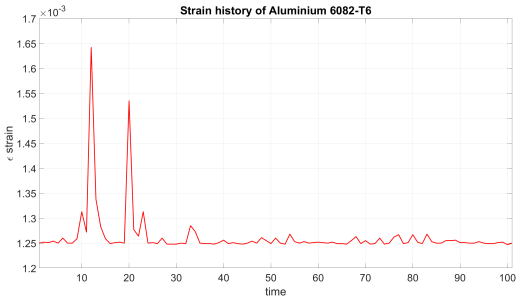

This one is when the material chosen is Aluminium.

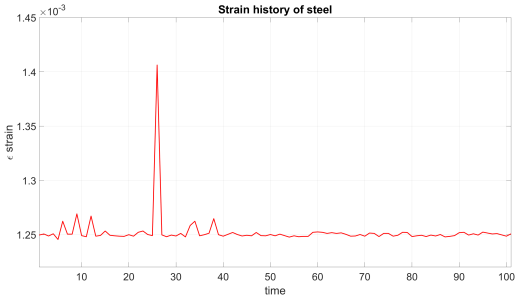

This on instead is the behavior if the material is Steel.

Rainflow Counting method

In order to reduce the number of value of strain the rainflow counting method is used.
The higher column represent the value of strain that occur many times.

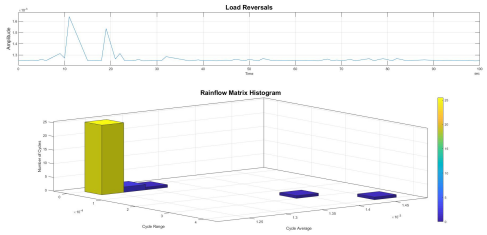

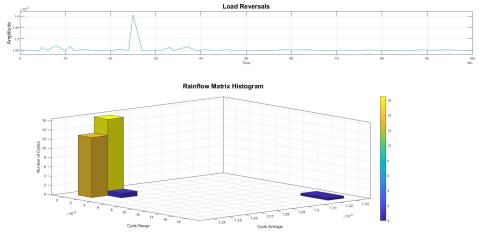

Morrow's Equation - Type C

After running the simulation we got the value of the strain amplitude so if we look for the cross point of the morrow equation and this value of strain amplitude we obtain the expected life of the component.

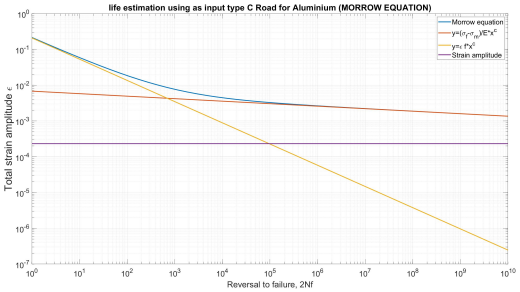

For The aluminium the Strain amplitude is 2.320e-4 and so the expectect life is infinite.

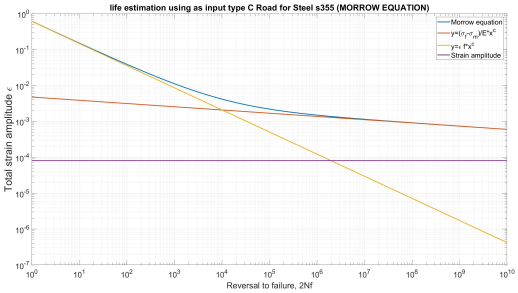

For the steel the Strain amplitude is equal to 8.038E-05 and also for this the expected life is infinite.

Smith-Watson-Topper's Equation - Type C

To do a comparison we use another method to evaluate the life of component the so called Smith-Watson-Topper's Equation. The idea is similar when the curve is crossed that is the expected life of the component.

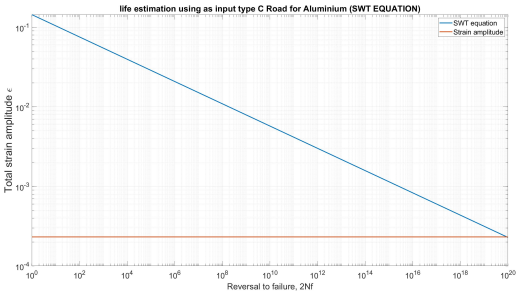

For The aluminium the Strain amplitude is 2.320e-4 and so the expectect life is infinite.

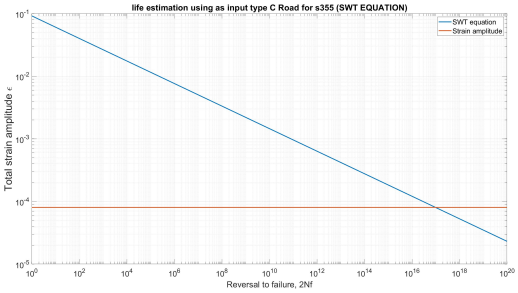

For the steel the Strain amplitude is equal to 8.038E-05 and also for this the expected life is infinite.

Road Bump

For this input I Simulated the different bump at different speed: 50Km/h, 80 Km/h and 120 Km/h.

Morrow's Equation - Road Bump

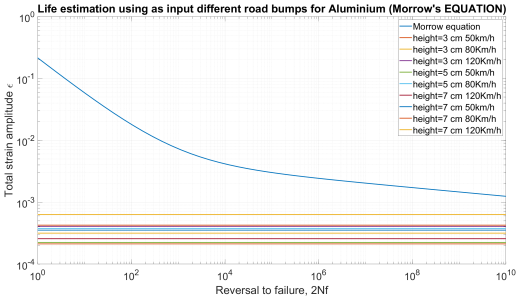

As can be seen the life expected for all the test is infinite.

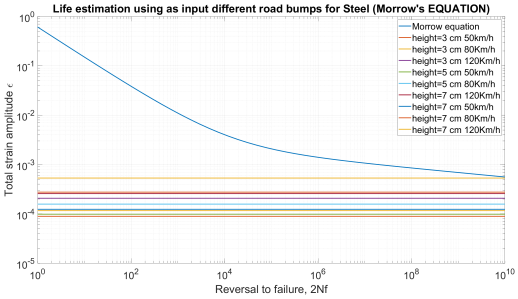

The same can be said when the material is steel.

Smith-Watson-Topper's Equation - Road Bump

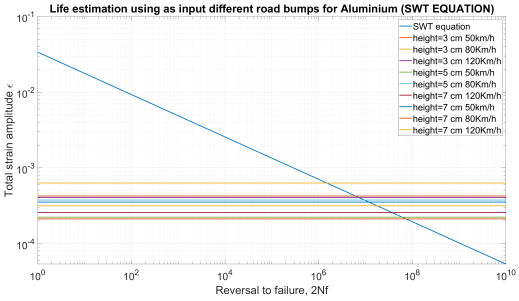

Here can be seen the life is not infinite, this happens because in the evaluation of the life, the max stress is considered and so the curve change.

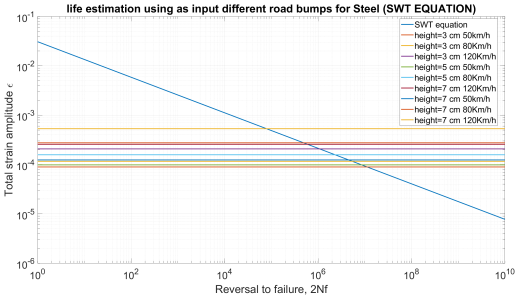

The same can be said when the material is steel.

Chapter 5

Conclusions

This method differs one from the other because the Morrow's Equation considers the mean stress, instead the Smith-Watson-Topper's Equation considers the max stress that sometimes can be so high that changes the life of the component. So in Conclusion can be said that the Smith-Watson-Topper's Equation is more conservative. The two method are equally usefull they must be chosen considering all the variable that take part the event. For the comparison of the material obviously steel performs better, but the aluminiun is much lighter, but it is very expensive. In my opinion the right choice is Steel.